

HISTOCHEMICAL STUDIES OF MUCOPOLYSACCHARIDES
IN EXPERIMENTAL MYELOSCHISIS

by

Stuart Dudley Wilson, B.S.

A THESIS
Presented to the Department of Anatomy
and the Graduate Division of the University of Oregon Medical School
in partial fulfillment of
the requirements for the degree of
Master of Science

May, 1964

Acknowledgments

My sincere gratitude to Dr. Robert L. Bacon, whose counsel, assistance, and enthusiasm over the past two years were greatly appreciated and a great aid in the completion of this work.

I also wish to thank Dr. David L. Gunberg, who gave me the opportunity to participate in this program and under whose direction this study was initiated.

And, finally, I wish to express my fond appreciation for the patience, encouragement, and assistance put forth by my wife, Jane, thus enabling me to complete this study.

TABLE OF CONTENTS

DIVISION	Page
I. INTRODUCTION	1
II. MATERIALS AND METHODS	14
III. RESULTS	23
A. Normals	26
B. Experimentals	38
IV. DISCUSSION	55
V. SUMMARY AND CONCLUSION	64
VI. REFERENCES	67
VII. APPENDIX	
A. Staining Methods	72
B. Tables	76
C. Graphs	90
D. Plates	101

Introduction

Spina bifida is a lower axial skeletal lesion that, presumably, has been present in man since antiquity, but only during the past two hundred years do we find it described in scientific writings. The lesion has frequently been associated with variable degrees of neural tissue defects. These defects, myeloschisis and myelomeningocele in the human, were well described by Keiller (30) in 1922 and again by Patten (44) in 1953; and more recently, experimental production of these abnormalities was achieved in the mouse and rat newborn (2,11,12,16,19,53,60) (such as were described and produced by Warkany et al (54), using trypan blue injections). Thus, the morphological pattern of development has been well discussed; but of the two theories which propose to explain the changes, neither has been verified.

Though spina bifida cystica, etc., had been recognized for centuries, it was not until 1761 that Morgagni (39) presented the first theories of the origin of these defects. His hydromyelic theory was based on the belief that the neural tube failed to close dorsally, due to increased cerebral spinal fluid pressure. "These watery tumors of the vertebra-" represented a disruption resulting from the pressure of fluid "descending in the tube of the spine" from the hydrocephalic head. This idea persisted unopposed until 1886 when von Recklinghausen (51) discredited it and proposed his own anaphic concept. On the basis of appearance alone, he felt the lesions were the result of an arrest in development and that the failure of the neural tube to close dorsally was not secondary to an increased cerebral spinal fluid pressure. Instead, he hypothesized that a primary neural tissue defect occurred prior to the

initial closure of the neural tube. A little over a half-century later, Patten (43) stated that he had observed in human embryos marked local overgrowth at the site of the defect and concluded that this overgrowth prevented the tube from closing. As his confirmatory evidence, he pointed to Fowler's (6) work in which the normally closed neural tube of chick embryos was mechanically slit dorsally and an overgrowth of neural tissue followed. Gardner (8, 9, 10) felt this to be an incorrect interpretation, for Fowler's work was done in the intact neural tube while Patten's observations were based on initially deformed material. Gardner related the development of the cystic lesion to a subsequent rupture of the neural tube, which, in turn, produced the secondary neural overgrowth. Cameron (4) also supported the secondary failure concept, but he felt the deformity resulted from an exaggeration of the physiologic hydroxyelia that Weed (58) observed during normal morphogenesis. This, Cameron hypothesized, would prevent the initial dorsal closure of the neural tube and neural arches. Thus, both the primary and secondary failure theories are still being disputed.

In reviewing these theories as to the method by which the defects are formed, I find that neither explanation can yet account for the range of lesions observed. Spina bifida is invariably present with meningocele, myelomeningocele, and myeloschisis. However, spina bifida occulta does not usually have an associated meningeal or neural lesion, as demonstrated by its presence in 15-20 per cent of the normal human population. As a consequence, we are faced with two forms of spina bifida: one most frequently purported to be a primary, isolated lesion without associated neural defects (occulta), and the other a secondary neural arch deformity associated with meningocele, myelomeningocele, and myeloschisis (44). To contribute to a unified graphic or primary failure

to close concept, I have attempted to approach the problem from a different point of view in this study.

It has been demonstrated that two mechanisms, the histogenic and the morphogenic, operate in normal axial skeletal chondrogenesis. In the context of this paper, histogenic refers to cellular acquisition (induction) of a differentiation potential; whereas morphogenic refers to the influences acting on these altered cells to create structural form and to establish morphological interrelationships with surrounding tissues. In this case, the histogenic inductor is a specific substance which can be isolated from the ventral half of the spinal cord. The substance presumably acts on receptive cells to induce them to secrete the vertebral cartilage matrix, which is chiefly composed of the acidic mucopolysaccharide chondroitin sulfate. It is hypothesized that an alteration in this induction system may lead to altered acid mucopolysaccharide elaboration during chondrogenesis, the end result perhaps being spina bifida and/or other vertebral deformities. In an attempt to verify this hypothesis, I have chosen myeloschisis for the experimental model.

In myeloschisis, the associated abnormalities in development of centrum and neural arch may be postulated as arising from two mechanisms. These are related to the alterations in the action of histogenic induction and of the morphogenic influences. It is assumed for this study that: 1) An alteration in the histogenic inductive mechanism will produce alterations in the biochemical development of the centrum and/or neural arch cartilage; and 2) an alteration in the factors (morphogenic) determining normal morphologic relationships between the vertebral elements and the spinal cord will not, by definition, produce alterations in the biochemical development of the cartilages.

In gathering support for these assumptions, I might begin by citing observations made by Patten (44). In the more severe forms of the deformities, he noted that the neural tube defects were established prior to the spina bifida deformity, i.e., when there were yet no indications of the neural arch primordia whatever. Around the notochord at this time, only suggestions of mesenchymal condensations were seen representing the primordia of the vertebral centra. Thus, primary neural tissue defects could be related embryologically to the development of axial skeletal defects.

During the past few years, further supportive evidence has arisen through the demonstration that a close relationship exists between the spinal cord and the subsequent development of normal vertebra. Studies have been done which show that the embryonic neural tube exerts the major influence in the induction of vertebra formation (5,14,23). This influence appears to act in two ways. The first is in the histogenesis of precartilag elements from sclerotomal cells. The second is the demonstration that the neural tube, spinal ganglia, and motor nerves have a significant bearing upon the form of the developing cartilage, i.e., morphogenesis. These two influences, apparently emanating from the spinal cord, appear to be the most prominent in vertebral development. Though the notochord plays a partial role in centrum formation, no evidence has yet been presented to show that it plays a role in neural arch formation.

These statements concerning the significant role of the spinal cord in neural arch formation are supported by studies performed on several different vertebrates, including *Amblystoma*, fish, chicks, and mice (15,21,55,57). In *Amblystoma*, it was shown that when a piece of spinal cord from 23- to 24-stage embryos was excised, vertebra failed to

develop in the cordless region (20). Some cartilage was noted to appear in the anterior and posterior portions of the operated region, but this was felt to be a result of caudal and cephalic sclerotomal migration of adjacent normally-induced cartilage centers. When the excised spinal cord was then grafted into the somites of a host (parallel to the host's spinal cord), a supernumerary vertebral column with neural arches from presumptive myoblast tissue was formed in all cases. All components of the induced system were morphologically identical to the normal host axial skeleton. When the medial three-fourths of such a group of somites (unilateral and bilateral, including the somite growth centers) were excised, normal neural arches still developed, but the dorsal, longitudinal musculature was markedly deficient.

Holtzer and Detwiler (22) have carried out further studies with *Amblystoma* to lend support to their previous conclusions that the urodele vertebral column is primarily induced by the spinal cord. Spinal cords in stage 37 embryos were split longitudinally along the midline, and three donor somites were then placed in between the two halves of the cord. Later, at four weeks after the yolk resorption stage, examination revealed that muscle and cartilaginous elements had formed between the two portions of the split cord. Each spinal cord was surrounded laterally by neural arches of their own, and medially by either an individual or, more frequently, a common neural arch. This dorsal neural arch system articulated with the appositional cartilage of the notochord. To demonstrate that the transplanted somites were undifferentiated at time of transplant, somites of the same stage donor were excised and implanted alone in the mesenchyme ventrolateral to a host's somitic mass. No cartilage or dorsal, longitudinal muscle was formed. These authors found that cartilage would form only if the donor spinal cord was included in

such a transplant. When another donor cord was implanted between the host's cord and somites number 6, 7, and 8 (with these shifted laterally), no cartilage developed to separate the two cords unless migratory mesenchymal components of the sclerotome had migrated between the two cords. In either case, the two cords were later encased by neural arches which assumed the contour of the cords.

Hotzer, Lash, and Holtzer (24) carried out experiments involving transplantation of 6-10 somites from tailbud *Amblystoma* embryos to the dorsal fin of young larval host embryos. When the somites alone were transplanted, examination 3-5 weeks later revealed that only small strands of muscle and pronephric tissue had formed; but implantation of the notochord along with the somite resulted in the formation of a small mass of muscle, irregular and inconstant cartilage mounds which adhered to the notochord, and scattered kidney tubules. Finally, when the somites were transplanted with a piece of spinal cord, there occurred a large mass of well differentiated muscle as well as cartilaginous vertebral elements (including precociously formed centra). That this spinal cord effect was not typical of all different types of neural tissue was demonstrated by co-transplantation of somites and forebrain. Examination of such transplant sites 3-4 weeks later revealed that only strands of muscle were present.

The fish embryo has also been the focus of some studies. Watterson (55), using the *Fundulus heteroclitus*, extirpated the neural tube from somites 4-14 and sacrificed the specimens when centrum and neural arch developments were evident at the unoperated levels. A complete absence of neural tissue typically resulted in no cartilage cells being found either lateral or dorsal to the notochord at the level of extirpation. Neural arches were found only when neural tissue was

encountered anterior and posterior to the excision site. If any neural tissue were left in the extirpated region, cartilage cells would form nearby. Associated, badly disorganized, nervous tissue served to demonstrate that relatively normal neural arches may form in relation to it. It was also noted that neural arches were complete in dorsoventral extent even though the dorsoventral extent of the cord was reduced. In the absence of the spinal cord, occasional small cartilage cell clusters lay dorsolateral to the notochord in the position of the bases of the neural arches.

The major studies in chick embryos have been carried out by Watterson, Fowler, and Fowler. (57) They demonstrated that partial extirpation of the neural tube resulted in a corresponding reduction in the dimensions of the vertebral canal. A decrease in the size of the neural tube produced decreased and thickened neural arches. Complete extirpation resulted in the absence of a vertebral column at the operative level. When this gap was small, the region between the free ends of neural tissue became filled with a solid cartilaginous rod. Complete removal of just one segment of spinal cord had this effect in the chick but not in the urodele. When the notochord was left behind, it was always enclosed by appositional cartilage, as in the urodele. Strudel (49) observed this in the chick also. His report states that vertebral cartilage was completely absent only when the notochord was also extirpated and when the ingrowing strands of neural tissue did not approach each other too closely. In retrospect, the investigators felt such results should have been expected; for in the earlier work of Wolff (62), description of degeneration of the neural tube and notochord was reported in the course of irradiating chick embryos. This, in turn, was accompanied by a reduced or absent vertebral column.

Lash et al (32), working with chick embryonic tissue cultures, confirmed these findings. They demonstrated that cartilage could be induced in cultures of chick somites only when spinal cord or notochord was present. In order to delimit the time of induction in chicks, a row of somites plus adjacent nephrotome were transplanted to the chorioallantois. In very young embryos (day 1), somite transplants resulted in no vertebral cartilage formation. 3-day-old donors formed cartilaginous rods or occasional vertebra-like masses. In 4-day-old donors, vertebra-like masses of cartilage were formed. The conclusion reached was similar to those from Holtzer's work with urodeles: Precartilaginous cells acquire their capacity for histological differentiation prior to the capacity for morphological differentiation. The same sequence has been seen with the mesenchymatous cores of limb buds of chick embryo cultures in vitro (57). However, this sequence has been disputed by Weiss and Amprino (59), who feel that the prescleral mesenchyme of the chick seems to acquire both the capacity for histological and morphological differentiation at the same time. In any case, somites definitely have been induced in urodeles after stage 35 (20) and, in the mouse, after 25 somites (15).

Few studies with mice have been recorded. An in vitro experiment has been carried out by Grobstein and Parker (15) in which they implanted clusters of six somites from 9-day mouse embryos into tissue culture media and found that the somitic tissue failed to differentiate into either muscle or cartilage. When cultured with a neural tube of the same stage embryo, the mesoderm differentiated into cartilage nodules. Grobstein and Holtzer (14) then performed in vitro studies of cartilage induction on mouse somite mesoderm. The spinal cords of 9-day mouse embryos were halved, and subsequently each half was independently

cultured in somite tissue. Of the 45 ventral-half cords, all but three formed cartilage; whereas, of the 20 dorsal-half cords, only one formed cartilage from the culture cord and mesoderm. Thus, it was concluded that the cartilage-promoting activity of the embryonic spinal cord is primarily located in the ventral half. When 9-day mouse somites were combined with fragments of spinal cord from successively older stages, a decline in the cartilage-promoting activity of the ventral spinal cord from 12- to 13-day-old embryos, and its disappearance in the 15-day-old, was noted. At no time was the dorsal one-half of the spinal cord significantly active. Also, they found no simple correlation between the mitotic activity or degree of neuron differentiation and cartilage-promoting activity of the spinal cord. Attempts at induction at various times with killed CNS tissue, other living and dead tissues, and inert materials were unsuccessful. Finally, by minimizing the area of contact between neural and somitic tissues in vitro, it was demonstrated that the inductive process of the neural tissue with the chondrifying cells is not necessarily contact-dependent.

Lash, Hommes, and Zilliken (33), interested in previous work performed by Holtzer that indicated the ventral half of the spinal cord possessed cartilage-inductive capabilities, initiated a study of the in vitro induction of vertebral cartilage in chicks. Using isolated chick somites, spinal cords, and notochords taken from 2.5- to 3-day incubates of stage 16- to 18-~~embryos~~ embryos (with the exception of some 4.5-day spinal cords used for extractions), cultures were made of inducing tissues (notochord and spinal cord), reacting tissues (somites), and chondrogenic cultures (inducing plus reacting tissues). A cold perchloric acid extract of ventral half of the spinal cord and notochord was observed to simulate the inducing actions of both of these intact

structures in vitro, i.e., inducing the formation of cartilage in explanted somites. Out of 228 cultures of the explanted somites, 186 developed cartilage when exposed to the extracted inducing substance. Cartilage usually developed within four days after the inducer was applied. In control somites, only 38 small nodules of cartilage were produced in 304 cultures. No inductive capacity could be attributed to extracts of the dorsal half of the spinal cord or to the sugar phosphate extract also obtained from the inducing tissues. Electrophoretic and chromatographic studies have revealed this inductive property as belonging to a nucleotide-containing fraction. Partial purification of this fraction showed that the cartilage-inducing capability was restricted to one nucleotide-containing component.

Hommes, van Leeuwen, and Zilliken have further studied this factor and believe that column chromatography has

definitely identified cytidine monophosphate and the amino acids aspartic acid, threonine, serine, glutamic acid, glycine, alanine, and valine in different ratios, and in addition a reducing hexosamine. Besides a cytidine nucleotide, spectral evidence shows the presence of a guanosine nucleotide. (25)

This complex is what I refer to in this paper as the histogenic induction factor(s). No indication was given in either of these studies as to the mechanism of the morphogenic relationship between the spinal cord and the developing cartilage.

In the studies mentioned earlier, portions were concerned with the spinal cord and its relationship to the diameter of the spinal canal, the morphology of the vertebral column, and the distance of the neural arches from the neural cord. Attention was first drawn to the relationship between the spinal cord morphology and the neural arch contour by Holtzer (20) in 1952. Studying urodeles, he found that the cartilage

formed around the cord and followed both normal and abnormal contours. As a corollary finding he also observed that the precartilage cells always maintained a characteristic distance from the cord and that the diameter of the spinal canal was dependent upon the diameter of the spinal cord. This was demonstrated by increasing or decreasing the amount of cord tissue, which resulted in a proportional adjustment in the size of the spinal canal. A critical amount of neural tissue, approximately 25 per cent of its normal value, was discovered to be prerequisite to normal molding of the vertebra and its processes; for when the amount of neural tissue fell below an apparently critical level of 25 per cent, vertebral arch formation was highly variable. In the complete absence of neural tissue before stage 36 urodele, the vertebra would not be formed. However, by this stage the precartilage cells of the trunk were determined, and they still formed a simple type of cartilage although all neural tissue was absent. This simple cartilage took the form of a dorsally located, solid, continuous, cartilaginous rod with periodic ventral extensions articulating with the notochord. Thus a distinct relationship between spinal cord morphology and neural arch morphogenesis was demonstrated.

Watterson and Spiroff (56) experimentally decreased the dimension of the lumbosacral level in the spinal cord of chick embryos by unilateral or bilateral leg bud extirpation. This resulted in a corresponding reduction in the dimensions of the vertebral canal. They also discovered that modifications in the spinal cord's shape were unusually reflected by corresponding modifications in the shape of the vertebral canal.

Each of the studies cited has served to point up the important role of the vertebrate spinal cord in axial skeleton formation. To re-

capitulate briefly, it was shown in *Amblystoma*, fish, and chicks, that early extirpation of the neural tube resulted in vertebral agenesis or dysgenesis. On the other hand, transplanting *Amblystoma* and chick neural tubes into somites *in vitro* led to formation of relatively normal vertebral elements surrounding the neural tissue. In *Amblystoma*, when somites were transplanted to a site between the spinal cord split longitudinally along the midline, formation of muscle and cartilaginous elements occurred. These cartilaginous elements assumed the contours of the surrounding neural tissues as well as articulating with the centrum below. However, if two segments of *Amblystoma* spinal cord were placed in direct contact (side by side) *in vivo*, no cartilage or muscle would form unless mesenchymal elements had migrated into the intervening area.

In vitro culture studies utilizing chick embryonic tissues demonstrated that cultured somites developed cartilage only when the spinal cord or the notochord was included in the culture. Using similar culture techniques, the actual time of somite induction in chicks was shown to be separate from the later time (3 days) of morphogenesis of cartilage. In somite cultures from mouse embryos, this inductive activity was related to the ventral portions of the spinal cord, and perchloric acid extractions from chick neural tubes and notochord proved to be chondrogenic when applied to receptive somites in culture.

These evidences of a biochemical interrelationship between the ventral portions of the spinal cord and the receptive centrum and neural arch precartilaginous sclerotomal cells appears to be one of major importance in axial skeletal development. I referred earlier to these inductive influences as histogenic. We have also seen that the morphology of the vertebra is chiefly dependent upon spinal cord morphology. No experimental evidence has been presented indicating that separate factors

mediate the cord's influence on vertebral morphology and spatial relationship to the vertebra. However, I have referred to those factors attending this relationship as morphogenic.

In conclusion, the histogenic and morphogenic influences are the major determinants in normal, and presumably abnormal, neural arch and centrum formation. Though the morphogenic factor influences the abnormal position and form of the vertebra in myeloschisis, by definition this influence would not participate in the biochemical process of chondrogenesis. As such, it is the histogenic inductive mechanism which forms the basis for this study, the hypothesis being that an alteration in the histogenic inductive system may lead to altered acid mucopolysaccharide elaboration during chondrogenesis. This will be accomplished by a two-phase study:

1. By the employment of histochemical methods for the study of complex acid mucopolysaccharides, mucoprotein, glycoproteins, glycogen and neutral mucopolysaccharides, the normal pattern of polysaccharide elaboration in the developing centra and neural arches will be studied.

2. By the application of these same histochemical methods to animals with the myeloschisis deformity, the altered histogenic induction hypothesis will be tested relative to the normal animals.

Materials and Methods

Rats of the Sprague-Dawley strain were maintained on a standard Purina rodent chow with Abdec^R vitamin supplements and sulfamerazine added to the water supply. Random mating of primiparous females for a period of two hours (± 1 hour) each day in an inverted light-cycle room produced adequate numbers of offspring for the study. At 9 days, 17 hours (± 1 hour) of gestation, the mother was given an intraperitoneal injection of 1 per cent aqueous trypan blue solution (the dye injection was fraction II blue, obtained from the crude commercial dye by column chromatography). The fetuses were collected on the desired days (13 through 18, ± 1 hour) while the mother was anesthetized. With each fetus, wet weight and crown-rump measurements were taken. After this procedure, each was immediately immersed in cold buffered-neutral formalin for 16-20 hours (37). Following fixation, dehydration in graded alcohols and clearing in xylene were carried out at room temperature. The specimens were vacuum-infiltrated with paraffin for 40-60 minutes at a maximum temperature of 65°C. and finally embedded. The blocks were sectioned at 10 microns, and every section was mounted serially on five sets of slides (i.e. each of the five sets included every fifth section serially following the corresponding section on the preceding slide).

Histochemical techniques demonstrating the presence of acid mucopolysaccharides and mucoprotein, glycoproteins, glycogen and neutral mucopolysaccharides were applied to the five parallel sets of mounted embryos, each staining procedure being carried out on the respective tissues at single sittings. The three techniques used to demonstrate the presence of acidic mucopolysaccharides were the Hale reaction and the Hale reaction control (after Mowry), the alcian blue

method (after Mowry), and the cresyl violet procedure (modified from Kramer and Windrum). Demonstration of the neutral mucopolysaccharides was accomplished by employing the periodic acid-Schiff reaction (after Mowry). Fetuses from noninjected mothers were prepared and stained by the same methods and were used for the normal study as well as for controls in the experimental study. The following briefly describes the basis for my using each technique.

Hale Reaction for Complex Carbohydrates with Free Acidic Groups:

In the original Hale stain (13), sections were placed in a 2 M acetic acid solution containing an equal amount of dialyzed ferric hydroxide; they were rinsed and then stained for ferric iron by the application of a solution of equal amounts of 0.14 M hydrochloric acid and 0.02 M potassium ferrocyanide. The resulting Prussian blue coloration, which appeared after application of the latter mixed solution, was said to demonstrate ferric iron combined with the acidic polysaccharides. However, specificity of this reaction was questioned by Kramer (28), who noted positive reactions with polyuronides, polysaccharide sulphuric acid esters, polynucleotides, phosphoproteins, and phospholipids. Later, Muller (42) reported that ferric oxide sol (made instantly by pouring ferric chloride into boiling water) could be used in place of dialyzed iron for this procedure. By employing this new preparation, Mowry (40) was able to develop a modified Hale-type procedure with increased sensitivity and selectivity. He subsequently reported that two deficiencies in his method had been corrected; namely, 1) variability in the depth of coloration appearing in duplicate sections stained with the same solutions at different times, and 2) the staining of background and cell cytoplasm. Variable but incomplete reversal of stock colloidal ferric oxide to

ferric chloride upon storage was thought to cause the color variability. This reversal was associated with increased hydrochloric acid formed in preparing the sol by hydrolysis. By dialysing this acid out of the freshly prepared ferric oxide sol for 24 hours, prolonged stability of the iron solution and decreased nonspecific background staining were achieved. Mowry also noted that the coloring appeared to correlate more closely with the distribution of the acidic carbohydrates when the pH of the staining solution was more acidic; therefore, enough glacial acetic acid was introduced into the working solution to acidify to pH 1.6-1.9. Finally, he found that background staining was effectively reduced without affecting the sites containing acidic carbohydrates when several rinses of 25-30 per cent acetic acid (same strength as the working solution) were applied. Thus, Mowry was able to achieve improved constancy and selectivity by 1) dialysis of the colloidal iron solution, 2) lowering the working solution pH with acetic acid, 3) employing an acetic acid rinse, and 4) preparing control sections to demonstrate aberrant ferric iron deposits.

Alcian Blue Stain for Complex Carbohydrates with Free Acidic

Groups: Alcian blue 8GS was first introduced in 1950 as a new stain for mucin by Steedman (48). He felt that the stain's specificity, clarity, and stability were good when using the proper method; but he acknowledged the possibility that other substances besides the mucins might be colored if the solution were applied to the tissue sections long enough.

Since the manufacturer has not yet made the information available, the exact chemical nature of the dye remains a trade secret. However, it is known to be an amphoteric dye which is a water-soluble derivative of copper phthalocyanin. The dye properties are believed to result from

thiourenium or pyridinium groups attached to this parent compound (17).

Vialli (50) observed that the staining pattern resembled that of toluidine blue metachromasia and thereby confirmed its use as a mucin stain. By using from 0.025 to 0.5 per cent alcian blue in pH 2.6 buffer, Rizzoli (46) observed that the enhanced selectivity of the dye appeared to be dependent upon the acid pH of the staining solution. He further noted that: 1) hyaluronic acid, chondroitin sulfate, and heparin applied to filter paper became stainable with alcian blue; 2) glycogen oxidized by periodic acid and then treated with sodium bisulfate was stainable; 3) methylation of tissues abolished the stainability of the mucopolysaccharides with alcian blue; 4) acetylation of tissues reduced but did not abolish the reactivity with alcian blue. The second observation in the above list presumably relates to the sulfonic groups (acidic) formed from bisulfite addition to aldehydes. It has also been found that alcian blue will color capsules of C. neoformans known to contain carboxyl but not sulfate groups (41, 6). The third and fourth observations are assumed to be based upon procedures that alter free acidic groups, (i.e. carboxyl) of the complex carbohydrates, thus blocking the reactivity to the dye. Mowry (40) felt that staining by the original procedure was not highly selective, but that the dye's contrast and sensitivity for acid mucopolysaccharides were enhanced by decreasing the concentration of the solution to 0.1 per cent in addition to lowering the pH from 2.7 to 3.0 with acetic acid. Wagner and Shapiro (52) reported that filas made of chondroitin sulfate, hyaluronic acid (heparin and umbilical cord), and vitreous humor all stained with the dye; whereas fibrin, albumin, and globulin did not color. They also demonstrated that the best pH range for dye binding specificity was from 2.3 to 2.8. Their conclusion was that alcian blue still lacked the sensitivity and selectivity to

be relied upon completely. Mowry (40) likewise stated that although the dye reaction strongly suggested the presence of acidic carbohydrates, the Hale technique should be used as an independent confirmation; and vice versa, the Hale technique should be verified by the alcian blue technique to confirm those features of cells and tissues revealed to be Hale-positive but not shown to be definitely metachromatic when stained with toluidine blue.

Thus far, all of the work discussed in this section has been carried out with alcian blue 868. Recently, however, a different form of the dye came into use; and it is this new form, 86X-300, which has been employed in the present study. According to Mowry, the results excel those of the earlier dye lots (40).

Cresyl Violet Stain for Complex Acid Carbohydrates: Cresyl violet, a thiazine dye, produces a metachromatic staining reaction in tissues containing acid materials of high molecular weight. Metachromasia has been defined as an alteration from the absorption spectrum of the original dye to that of the tissue-dye complex, thus producing the altered color; therefore, in the case of cresyl violet, the blue staining of the original dye is altered to a magenta or violet color when combined with structures containing metachromatically reactive substances.

The essence of the metachromatic reaction has not been well defined experimentally, but theoretical discussions summarized by Pearse (45) have indicated that "metachromasia signifies only the presence of free electro-negative surface charges of certain minimum density" on the substrate. Thus, the substrate molecule is believed to act as a center of orientation which attracts, by means of its free anionic groups, the polar groups of the dye-stuff (47). This is the primary requirement

for the metachromatic reaction. The secondary requirement is related to the surface density of negative charges on the substrate; that is, increased metachromatic intensity has been shown to occur as SO_3H group density per disaccharide unit of a polysaccharide increases (45). Sylven, as cited by Pearse (45), disagrees with this concept of metachromasia. His position is that secondary new high-energy bonding (van der Waal's forces) between the aggregated dye molecules leads to the spectral shifts manifested as metachromasia in stained tissues. Despite the theoretical discussion that still persists on the mechanism of this reaction, the metachromatic staining of acidic mucopolysaccharides by these dyes is generally accepted.

Previous investigators have found that the metachromasia exhibited by mucous cells and many ground substances is due to the mucopolysaccharides (38,61). However, as Michaelis (38) has pointed out earlier, not all metachromasia is referable to the mucopolysaccharides, for nucleoproteins and substances of unknown composition stained metachromatically under certain conditions. Wislocki, Bunting, and Dempsey (61) discovered that some of the extraneous stained substances were ribonuclease-sensitive, while other, faintly metachromatic, extraneous reactions could be reduced by initial fixation with 10 per cent neutral-formalin. Using the thiazine dye toluidin blue, they found metachromasia to be very intense in fibrocartilage matrix and other tissues known to contain basophilic acid sulfate groups. That such staining was not entirely dependent upon the sulfate linkage was demonstrated by the metachromatic staining of another acid mucopolysaccharide, hyaluronic acid. They employed toluidin blue in staining the ground substance of cartilage and found metachromatic staining to be stronger in the perilacunar

than in the interlacunar portion of the hyalin matrix. This corresponded with the distribution of basophilia. Only the perilacunar region remained metachromatic to toluidin blue when the cartilage matrix was subjected to low pH, 1.5-3.0 (thereby increasing specificity of the technique); whereas both portions of the cartilage ground substance stained the same at pH 5-7.

Because its metachromatic contrast is better than that of toluidin blue, cresyl violet (at low pH) has been used in the present study. Also, the metachromatic staining reaction of cresyl violet is more stable for storage over longer periods of time than that of toluidin blue.

Periodic Acid-Schiff for Complex Carbohydrates: Jackson and Hudson (29) in 1937 were the first definitely to show periodic acid's ability to quantitatively oxidize carbohydrates (starch and cellulose), while McManus (36) in 1946 became the first to describe its use in the histological demonstration of mucins. McManus's report stated that fixed tissues were, first of all, brought to water and treated with periodic acid; then they were washed briefly and placed in Schiff's reagent. Following this, the sections were washed in sulphurous acid and afterwards dehydrated, cleared and mounted for study. The mucins of several tissues were found to be strongly colored as a result.

Using periodic acid, Schiff's reagent, and sodium bisulfite, Lillie (35) and Hotchkiss (27) elaborated the method, and the latter felt his method should derive positive results from any substance that fulfils the following criteria: 1) It must contain either a 1:2-glycol grouping (or the equivalent amino or alkylamine derivative) or the oxidation product CHOH-CO ; 2) it must not diffuse away during tissue fixation; 3) it should

give an oxidation product which is not diffusible; and 4) it must be present in sufficient concentration to give a detectable final color. In animal tissue, the naturally occurring substances able to give positive results and thus fulfil these criteria were monosaccharides, polysaccharides, mucoproteins, glycoproteins, phosphorylated sugars, cerebositides, and inositol-containing lipids. However, after fixation, dehydration, clearing, and infiltrating with paraffin, the only substances which remained in the tissues to give a positive reaction were polysaccharides, hyaluronic acid, mucoproteins, and mucins.

LeBlond et al (34) carried out extraction studies on tissue and secretions known to react variously to the periodic acid-Schiff procedure. Fraction I of their extracts, which was known to contain the acidic mucopolysaccharides, was PAS-negative; but fraction II, containing hexoses, fucose, hexosamines, and sialic acid, was strongly positive. It was found that the hexose content of these substances closely paralleled the intensity of PAS staining in paraffin sections. Uronic acid (no 1:2-glycol groups) was not found to be present in the chemical determinations.

In determining the hexose content of reticulin and collagenous fibers, Glegg et al (13) found that both materials contained the same four sugars: galactose, glucose, mannose, and fucose. The quantitative amount of each of the hexoses paralleled the intensity of PAS staining, the reticulin fibers containing significantly more (as well as being more intensely colored) than the collagen fibers. In vitro tests carried out by Braden (3) confirmed the fact that the acid mucopolysaccharides do not support the PAS reaction. He studied preparations of hyaluronic acid, chondroitin sulfate, heparin, the acidic mucopolysaccharides from cornea, gastric mucin and dentine, and the neutral mucopolysaccharides

from gastric mucin. With the exception of the dentine preparation, the acid mucopolysaccharides stained only weakly, while the neutral mucopolysaccharides colored intensely. The acidic mucopolysaccharides were found to react positively to toluidine blue and the original Hale stain.

Hooghwinkel and Smits (26) observed likewise that hyaluronic acid and chondroitinsulphuric acid in vitro did not color with the periodic acid-Schiff reaction. In conclusion, it is generally believed that the PAS techniques only demonstrate the presence of 1:2 glycol (and alpha-aminoalcohol) groups in tissues.

Results

A total of 23 fetuses with the deformity were prepared for study. Twelve were found to support the hypothesis; however, four others did not appear to uphold it. Three of the latter were 18-day-old fetuses, and one was 16-days-old. The remaining seven deformed fetuses were non-contributory to the study due to technical difficulties. Of the 12 fetuses supporting the hypothesis, 8 will be presented in the text. Two more fetuses, each 15-days-old, were similar to the 15-day embryos already chosen for presentation, and on this basis are not reported in detail. Another 14-day-old animal demonstrated no alteration in sub-spinal mesenchyme or neural arch matrix staining even though a well defined myeloschisis deformity was obvious. And, finally, a 15-day-old fetus demonstrated disruption of the spinal cord without classical myeloschisis or spina bifida cystica defects being formed. In succeeding caudal levels, the spinal cord was represented by sporadic neural tissues in the dorsal portions of the animal. Some of these masses were accompanied by staining of the surrounding mesenchyme, and in these instances, surrounding cartilages were observed to have formed.

The normal control study was supported by detailed descriptions and data tabulations of one representative embryo for each day. The resultant pattern of mucopolysaccharide distribution was confirmed by subsequent study of 27 normal fetuses, as tabulated in Table XIV. The normal or control study represented an attempt to define the cartilage matrix morphology and histochemical properties at a representative level (anterior portion of the posterior limb buds). It also served to summarize the histochemical properties at several normal levels with which were compared the levels in malformed fetuses where the lesions occurred.

These normal levels have been represented by the Roman numerals I through VI, corresponding to selected paraxial structures that serve as landmarks. The paraxial structures and the normal reading levels were both related to ranges of approximate vertebral levels summarized in Table I. Table II correlates the reading levels (I through VI) in the normal animals with the lesion levels (1 through 5, 6, or 7) of the experimental group. The normal readings are summarized for the 14-, 15-, and 16-day fetuses in graphs 3, 6, and 9 respectively. However, to relate these data to the graphic patterns of experimental data, Tables I and II must be simultaneously studied to determine which of the normal reading values applies to the particular lesion level where the experimental reading was taken. It must be remembered that the staining values presented cannot be applied as a measure of quantitative variations between fetuses, and, as such, the data are limited to determining in each fetus the pattern of mucopolysaccharides at progressively more caudal levels. Only the data pertaining to the acidic mucopolysaccharides in the abnormal and normal neural arches and subspinal cord mesenchyme have been presented in graphic form. In both groups of animals the data were collected from levels separated from other levels by varying and unequal distances. As such, the graphic representation does not infer equal intervals between plotted values. The ratings were based on a subjective scale from zero to 4+, which was devised as a summary evaluation of three staining parameters: density, intensity, and quality. Therefore, this rating system represented an approximation gained from visual inspection. Quantitative comparisons between specimens could not be made because of variability in staining. The usefulness of the system was in the comparison of the relative staining qualities of structures at different levels in any one fetus.

Plates, tables, and graphs were used throughout the results and discussion and were interrelated in the text. In particular, Plate 7 is composed of normal 14-, 15-, and 16-day-old fetuses for comparison with cross-sections of deformed animals to be described.

Finally, in the text and tables a system of abbreviations for the histochemical methods is used, as follows: Hale = Hale reaction; AB = alcian blue staining reaction; CV = cresyl violet staining reaction; and PAS = periodic acid-Schiff staining reaction. Each of these stained characteristically: Hale reaction = blue; alcian blue = turquoise green; cresyl violet = pink to magenta; and periodic acid-Schiff = pink to magenta.

I. The development and distribution of acidic mucopolysaccharide and PAS-positive material in the developing normal posterior axial skeleton.

A. Prior to the thirteenth day: Classical embryological description depicted the origins of the post-cranial axial skeleton as resulting from medial migration of the paraxial proliferating somitic cells, the embryonic mesoblasts. The cells were derived from the inner cell mass of the embryonic disc. As the primitive streak formed caudally and extended cranially, the mesoderm spread laterally over the disc parallel to the streak's course. When the primitive knot was formed and the notochord continued to grow cranially, the mesoderm likewise continued to sweep cranially and laterally alongside this structure between the primitive ectoderm above and entoderm below. Segmentation of the mesoderm took place, and soon, following the primary somite formation, secondary subdivisions occurred, forming the lateral dermatomic, central myotomic, and medial sclerotomic cellular accumulations. The myotome and sclerotome were separated by a cavity, the myocele. Early migrant cells could now

be seen to extend medially from the sclerotome toward the centrally placed notochord (which lay ventral to the neural tube). It is at this point that the present study commences.

B. Thirteen-day-old fetus: N13-10. Fertilization age 13 days \pm 1 hour. Crown-rump length 0.84 cm. Wet weight 69.6 mgm. Cross-sectioned. Good preservation with minimal variability in staining between sections.

Caudal to the anterior margins of the posterior limb buds, no definitive cartilage cells were present in the regions of the future centra or neural arches. Sclerotomal cells migrated medially as flow patterns from the lateral somitic mass. Centrally, these cells formed segmentally arranged cell aggregates located on either side of the notochord; in the intersegmental regions destined to become centra, the mesenchymal cells showed no change from the primitive state. Both the intercellular spaces of the segmental and the intersegmental regions stained equally for acidic mucopolysaccharides on fine, fiber-like structures.

The sclerotomal cell migrations also formed aggregates in the regions of the future neural arches. These cells remained undifferentiated and formed a polarized flow laterally, sweeping in a ventral-to-dorsal direction around the spinal cord. The intercellular portions of this cellular flow colored variably with the Hale and alcian blue reactions, the strongest site (2+) occurring ventromedially to the respective dorsal root ganglion. However, no distinct nidus of precartilage formation was present. Cresyl violet was minimally metachromatic (1+) in the fine, intercellular, fiber-like processes extending between the cells. In the same region, periodic acid-Schiff staining was absent.

The intervening mesenchyme between the spinal cord and the

centra and neural arches was very lightly colored. The intercellular portions of the notochord were stained PAS-positive (2+). The perinotochordal region was markedly stained (Hale 1+; AB 3+; CV 2+; PAS 0) while the central notochord was unstained. No beading of the notochord was yet apparent. The spinal cord and ganglia were unstained.

C. Fourteen-day-old fetus: N14₁-6. Fertilization age 14 days 1 hour, \pm 1 hour. Crown-rump length 1.02 cm. Wet weight 123.8 mgm. Cross-sectioned. Good preservation with little variability in staining between sections.

Caudal to the anterior margins of the posterior limb buds, no early cartilage cells were discerned in the regions of the future centra or neural arches. At the levels of the anterior portion of the posterior limb buds, the region of the intercentrum (segmental) and the region of the future centrum (intersegmental) stained intercellularly. As compared to the 13-day-old fetus, the sclerotomal cells were more condensed in the region of the future neural arches lateral to the spinal ganglia. However, the intensity of the intercellular staining in this region increased and extended further dorsally than before. The intercellular precartilaginous matrix varied in structure with different stain techniques employed.

In the preneural arch region, the Hale reaction and alcian blue stain demonstrated fiber-like structures (Hale 2+; AB 1+) intermingling with a background of stained, irregularly shaped aggregates of granular material (Hale 2+; AB 1+). Cresyl violet did not stain the preneural arch matrix. The stained areas did not terminate at the margins of the intensely stained regions but extended dorsally into a group of cells migrating over the spinal cord. The PAS-positive coloring appeared as randomly occurring, discrete, large but irregularly shaped, homogeneous

deposits in the intercellular spaces (1+). The mesenchymal tissue ventral to the spinal cord again exhibited coloring, and the notochord remained in its cylindrical form without evidences of segmental beading. Intercellular staining of notochord was only PAS-positive (2+) while the perinotochordal region stained with Hale (2+), alcian blue (3+), and cresyl violet (2+). A small, round, central core in the notochord was present both segmentally and intersegmentally, and it could be identified by alcian blue (2+) and cresyl violet (2+). The spinal cord and ganglia were not stained.

Staining values taken at several reading levels are recorded in Table III. Histogram 3 demonstrates that the normal staining patterns exhibited by the three acidic mucopolysaccharide reactions were identical at reading levels II, III, and IV for the subspinal cord mesenchyme (Hale 2+; AB 2+; CV 1+) and the preneural arch matrix (Hale 2+; AB 1+; CV 0). At reading level V, the subspinal cord mesenchyme remained unchanged (Hale 2+; AB 2+; CV 1+), whereas the preneural arch matrix stained with less intensity (Hale 1+; AB 0; CV 0).

D. Fifteen-day-old fetus: N154-6. Fertilization age 15 days \pm 1 hour. Crown-rump length 1.28 cm. Wet weight 245.6 mgm. Cross-sectioned. Good preservation with minimal variation in staining between sections.

Caudal to the anterior margins of the posterior limb buds, cartilage of early neural arch and centrum was well formed. At the levels of the anterior portion of the posterior limb buds, the centrum exhibited strong intercellular staining. Likewise, the stained neural arches of the early cartilaginous masses did not extend dorsally beyond a horizontal line drawn between the ventral third and the dorsal two-thirds of the spinal cord, bisecting the ganglia. The cartilaginous neural arches were

in direct continuity with the centrum, and the overlying subspinal cord mesenchyme was colored. The matrix of the neural arch and the centra were prominently stained, but regional variation within each cartilage body occurred for the first time. With the Hale reaction (Figure 1A), bands composed of many deeply stained, fine, fiber-like threads coursed between the cellular structures. These bands were accompanied by small aggregates of intensely stained granules, which, in turn, lay upon a background of small, fine granules and fiber-like structures that stained less intensely. The lacunar spaces were not distinct from the contained cells.

Alcian blue (Figure 1-B) demonstrated an almost homogeneous, well stained background with colored, fine, fiber-like structures in the matrix. The lacunae were better defined than with the Hale reaction.

Cresyl violet (Figure 1-C) also demonstrated narrow bundles of fine, fiber-like material on a background of finely granular material which stained only slightly less intensely than the bundles. The lacunar spaces could be discerned with this method.

The PAS reaction (Figure 1-D) demonstrated no significant matrix coloring, but small intercellular deposits of PAS-positive material (3+) were present. Again, the lacunar spaces could not be well differentiated from the contained cells.

None of the techniques demonstrated a well defined perichordrium. The notochord (Figure 3-A) displayed no beading, and the vertebral (inter-segmental) and intervertebral (segmental) portions stained alike: intercellular (Hale 0; AB 0; CV 0; PAS 3+); central core (Hale 0; AB 4+; CV 4+; PAS 1+); perinotochordal region (Hale 2+; AB 4+; CV 4+; PAS 1+). The spinal cord and ganglia were unstained. The myotomes and ganglia were in their normal positions.

At the anterior segments of the posterior limb buds, a rapid transition from sclerotomal aggregates to early cartilage occurred between the fourteenth and fifteenth day. To fill this descriptive gap, the transition zone in the 15-day-old fetus was studied. Because this was located in the rump region, it presented in the frontal section, allowing for easy comparison of contiguous segments. The change from precartilage to cartilage matrix was represented by a progressive increase in staining for the acidie mucopolysaccharides. The change was not abrupt, and progressive alteration from a 14-day-old to a 15-day-old matrix pattern spread over four to five consecutive segments, proceeding caudal to cranial in direction. The neural arch transition zone was found to be two to three segments anterior to the centrum transition zone, a consistent pattern observed in all fetuses. In this transition region, the subspinal cord mesenchyme was well colored.

Staining values taken at several reading levels are recorded in Table IV. Histogram 6 demonstrates that normal staining patterns exhibited by the three acidie mucopolysaccharide reactions were identical at levels III, IV, and V for the subspinal cord mesenchyme (Hale 2+; AB 2+; CV 2+) and the neural arch matrix (Hale 4+; AB 4+; CV 3+). At reading level VI only one stain revealed change in the subspinal cord mesenchyme (Hale 2+; AB 2+; CV 1+), whereas the neural arch matrix stained less intensely with all three techniques (Hale 2+; AB 2+; CV 1+).

E. Sixteen-day-old fetus: N16₁₋₂. Fertilization age 16 days 2³/₄ hours, ± 1 hour. Crown-rump length 1.55 cm. Wet weight 382.8 mgm. Cross-sectioned. Good preservation with minimal variation in staining between sections.

At the anterior segments of the posterior limb buds, the centra and neural arch cartilages were well formed. The segmental intercentrum

cell aggregates were not stained. The cartilage matrix of the centra and the neural arches did not differ from each other, but regional variation within a single cartilage occurred. The neural arches extended dorsally to the level of a horizontal line which bisected the spinal cord into dorsal and ventral halves and lay at the dorsal aspect of the spinal ganglia. Ventromedially, each arch was in direct continuity with its centrum.

The Hale reaction, when applied to the neural arch matrix, disclosed a light blue, homogeneous-appearing background (3+) with prominent pleomorphic perilacunar granules (4+) and occasional pleomorphic matrix granules (4+). No fibers ran in the matrix, and the lacunar spaces could not be discerned from the cytoplasm of the enclosed cells. Intercellular staining extended into the region where cartilage was forming at the distal end of each neural arch. Otherwise, the cartilage was well delineated at its margins.

The portions with an alcian blue staining intensity of 4+ were associated with narrow, multiple, fiber-like accumulations forming single bundles which coursed between the cells in the matrix. Surrounding these were finer fiber-like lines with a coloration of 4+ on a less prominent, homogeneous-appearing background (3+). The portions with lacunar spaces were homogeneously stained. In the dorsal portions of the neural arches, the matrix differed by having a deeper homogeneous-looking background (4+) with no fine, fiber-like accumulations moving through it. The larger, intensely stained, fiber-like bundles remained as noted above (4+). The margins of the cartilage matrix showed gradual diminishment of coloration, but significant amounts occurred intercellularly in the migrating mass of cells extending dorsally over the cord.

Cresyl violet was more specifically restricted to the magenta-

colored, well formed portions of the cartilage. Many fiber-like accumulations made up larger, magenta-colored bands running through the matrix between the cells. These were set on a finely granular, pink background (1+). Relatively less mature, dorsally located, neural arch cartilage matrix consisted of similar heavy bands lying midway between the cells. These bands were made up of many fine fibers (4+ magenta). Meshing with these larger accumulations, fine isolated fibers (3+) coursed in a finely granular, deep pink (2+), intercellular matrix. The lacunar spaces did not color. In both the early and the older cartilage bodies, all matrix coloration diminished rapidly in intensity at the periphery of the cartilage, with neither magenta nor pink extending beyond the apposition cells or into the cells flowing toward the dorsum of the spinal cord.

PAS-staining was minimally distributed in the matrix (1+ pale pink). This matrix appeared homogeneous, and no fibrous structures were visible. The cell cytoplasm colored 3+ magenta, with some small, sporadic, granule-like accumulations being slightly the more prominent (3+). The areas of heavy cytoplasmic staining (3+) increased in density as the periphery of the cartilaginous mass was approached. The pericellular lacunar spaces were uncolored. Magenta coloring of small pleomorphic masses located intercellularly became noticeable in the appositional cell layers at the margins of the cartilage and among the cells extending dorsally over the spinal cord (4+).

Ventral to the spinal cord, the mesenchyme colored prominently (Hale 3+; AB 3+; CV 1+; PAS 3+). The lateral somites likewise exhibited intercellular staining (Hale 3+; AB 3+; CV 1+; PAS 4+) though this was less intense in other normal specimens. The notochord was beaded segmentally, and at the regions where the increased diameters were prominent, the staining was as follows: intercellular, (Hale 4+; AB 4+; CV 4+; PAS 0);

central core (Hale 0; AB 4+; CV 4+; PAS 0); perinotochordal region, (Hale 4+; AB 4+; CV 3+; PAS 0). Within the centra, notochord morphology remained unaltered. The staining characteristics were: intercellular (Hale 2+; AB 0; CV 0; PAS 4+); central core (Hale 0; AB 4+; CV 4+; PAS 0); perinotochordal region (Hale 4+; AB 4+; CV 3+; PAS 0). The spinal cord and ganglia were unstained.

Staining values taken at several reading levels are recorded in Table V. Histogram 9 demonstrates that the normal staining patterns exhibited by the three acidic mucopolysaccharide reaction were identical at reading levels II, III, IV, and V for the subspinal cord mesenchyme (Hale 3+; AB 3+; CV 2+) and the neural arch matrix (Hale 4+; AB 4+; CV 4+).

G. Seventeen-day-old fetus: N17₅-9. Fertilization age 17 days \pm 1 hour. Crown-rump length 1.71 cm. Wet weight 631.8 mgm. Cross-sectioned. Good preservation with minimal variation in staining between sections.

At the anterior segments of the posterior limb buds, the cartilage was well formed in both the centra and neural arches. The neural arches extended dorsally to a horizontal line drawn tangent to the dorsal surface of the spinal cord. The matrix morphology and staining were the same in both structures. Neural arch matrix stained prominently; however, the staining pattern was variable within each cartilage. The Hale reaction markedly colored the matrix. Heavy, irregular bands (3+) coursed between the lacunar spaces. At random sites the heavy bands appeared to have fragmented, leaving small granular islands and fine fibers (4+) supported on a homogeneous blue background (3+). The lacunar spaces were rated 3+, but the contained cells remained unstained. There was prominent perilacunar accentuation of stained granules (4+) seen

elsewhere in the matrix. The coloring did not extend beyond the well defined cartilage bodies except at the dorsal end where new cartilage was forming over the spinal cord (spotty intercellular 3+).

Alcian blue distinguished more prominently between the matrix background staining (3+) and the heavier interlacunar bands of fiber-like structures (4+). Bands of fine, fiber-like components were also present in the matrix but were not as prominent as in the 16-day-old fetus. The predominant component of the cartilage stained with alcian blue was the homogeneous portion of the heavier bands. The peripheral coloring was limited to the inner layers of the future perichondrium, and dorsally, where the neural arch cartilage was being newly formed to cover the spinal cord, less prominent staining occurred (gradation down to 1+ in the cell flow).

Cresyl violet staining was limited to cartilage of the neural arch and centrum and to the subspinal cord mesenchyme. A background of finely granular matrix was stained 3+, while prominently colored (4+) bundles of definitely fiber-like structures lay between the lacunar spaces. These bundles appeared to fragment and become less distinct or absent in the larger areas of matrix that were relatively devoid of cells. No staining of lacunar space appeared, and the cells did not color metachromatically. No staining occurred around the periphery of the cartilage. However, in the areas where new neural arch cartilage formed dorsally, color decreased rapidly.

The PAS reaction stained the matrix only minimally (1+). The cytoplasm of the cells contained pleomorphic accumulations of metachromatic material similar to those of the 18-day-old fetus to be described next.

The subspinal cord mesenchyme was stained prominently (Hale 3+;

AB 3+; CV 1+; PAS 1+). The segmental, widened portion of the beaded notochord stained in the following pattern: intercellular, Hale 4+, AB 4+, CV 0, PAS 4+; central core was absent; perinotochordal, Hale 4+, AB 4+, CV 4+, PAS 1+. The spinal cord and ganglia were unstained. The myotomes and ganglia were in their normal lateral positions.

H. Eighteen-day-old fetus: N18₁-10. Fertilization age 18 days 3 $\frac{1}{4}$ hours, \pm 1 hour. Crown-rump length 2.49 cm. Wet weight 1282.2 mgm. Cross-sectioned. Good preservation with minimal variation in staining between sections.

At the anterior segments of the posterior limb buds, vertebral cartilage was well formed. The centra and neural arches both demonstrated changes compatible with the early establishment of pre-ossification centers. Other regions were similar to the cartilage described for the 17-day-old fetus. The neural arches were in direct continuity with the centra below, and they extended dorsally and medially to cover partially the dorsolateral portions of the spinal cord. For the first time, a very definite sheath of spindle-shaped cells formed a perichondrium around the formed cartilage. The most distal portion of the neural arches rapidly changed from cartilage to precartilaginous elements in the short cell flow which interconnected the bilateral neural arches dorsal to the spinal cord.

The Hale reaction (Figure 2A) in the pre-ossification centers predominated in a perilacunar pattern (4+). Aside from these areas of irregular deposition around the immediate margins of the lacunar spaces, the homogeneous turquoise color was less intense than that seen in the 17-day-old fetus. The lacunar spaces and cells were devoid of stain. In more peripheral regions of the neural arch, the same distribution of stain was present. However, the density and amount of stainable material

had decreased. Only irregular 4+ deposition occurred around the immediate margins of the lacuna. The remainder of the homogeneous-appearing matrix colored a much lighter shade of turquoise (3+). No fiber-like aggregates of stained material filled the matrix. Near the dorsomedial portion of the neural arch, the transition region demonstrated heavy aggregates of stained material (4+) resembling a coarse precipitate that were irregularly distributed in a less prominently colored matrix (2+). The interconnecting flow of cells extending dorsally over the cord had small amounts of turquoise coloring (1+) intercellularly. Except in this transition region, the extent of the reaction was limited to the cartilage margins.

Regions of cellular degeneration in the neural arch showed the turquoise-green color of alcian blue (Figure 2B) to be most marked in the perilacunar area (4+). This appeared organized in a web-like manner between the cells on a background of homogeneous-appearing matrix (3+). Minimal staining took place in the lacunar spaces. The more peripheral, non-degenerating portions of the neural arch cartilage demonstrated a narrow margin of homogeneous-appearing, perilacunar coloring (4+). The more abundant, homogeneous-appearing, matrix background colored only slightly less intensely, still 4+. In the transition area (precartilage to cartilage), the intercellular region showed occasional fine, fiber-like, stainable material (4+) on a somewhat less intense, finely granular background (3+) between the more spindle-shaped cells. Some turquoise-green was present in the cell flow over the spinal cord (2+). The stainable tissue ended abruptly at the cartilage margins except in the transition area.

Between the lacunar spaces where degeneration of the chondrocytes occurred in the pre-ossification centers, cresyl violet (Figure 2C)

colored the matrix intensely (4+) in a web-like distribution. The more homogeneous background of matrix (3+) contained a few fine, filament-like structures (4+). Fine, reticular, interlaced structures occurred in a loose pattern surrounding the cells. The cells were devoid of coloring, as were the lacunar spaces. In more peripheral portions of the neural arch cartilage, the cells colored slightly (3+) and the lacunar spaces stained magenta (2+). The intercellular material appeared as a homogeneous background of magenta (4+) containing fine, filament-like structures (4+). In the transitional zone, metachromasia extended a short distance into the cell flow, diminishing rapidly in intensity. Elsewhere, staining continued only to the margins of the cartilage.

PAS metachromasia (Figure 2D) was again only slight in the matrix of the degenerating regions of the neural arch (1+). However, the degenerating cells contained many large, round and pleomorphic, metachromatic granules (4+). Toward the periphery of the cartilage, this material became progressively less distinct, less regular, and decreased in amount. In these more peripheral regions, the matrix remained the same (1+). The transition area demonstrated a gradual diminution of intercellular metachromasia and a gradual increase of small and pleomorphic, extracellular accumulations of metachromatic material (3+). The margins of the cartilage were not well defined by staining. The cell flow dorsal to the spinal cord stained 3+ intercellularly.

The subspinal cord mesenchyme stained less prominently than in younger fetuses (Hale 3+; AB 3+; CV 0; PAS 1+) and the reaction was limited to the region above the well defined meninges. The notochord divided into large, intervertebral expansions and smaller, degenerating, intracentrum aggregates which occasionally disappeared. The intervertebral portions stained as follows: intercellular, Hale 4+, AB 4+, CV 3+, PAS 4+;

the central core was essentially absent; perinotochordal, Hale 3+, AB 4+, CV 4+, PAS 0. The spinal cord and ganglia were unstained. The myotomes and ganglia remained in their normal lateral positions.

II. The distribution of acidic and neutral mucopolysaccharides in the developing, malformed, posterior axial skeleton.

A. Fourteen-day-old fetus: E1⁴₂-7. Fertilization age 14 days ± 1 hour. Crown-rump length 0.94 cm. Weight 137.4 mgm. Cross-sectioned. The fetal tissues were well preserved throughout processing with minimal histochemical staining variability between sections. A myeloschisis deformity was noted grossly, and on microscopic examination the deformity extended from the cranial portion of the posterior limb buds in the rump to a position caudal to the posterior limb buds. The region immediately cranial to the lesion showed no morphological or histochemical deviations from normal (lesion level 1).

The cranial portion of this lesion is represented by Figure 4A. This region (lesion level 2) was cut in frontal section, and beyond the level of the cutaneous tissue the defect appeared only as a dorsal extension of the spinal cord tissue. Its dorsal surface was denuded of epithelium and appeared to have undergone moderate degenerative changes. No other deviations could be observed within this section.

A few segments caudally (lesion level 3), the dorsal spinal root ganglia had coalesced in the midline while the spinal cord had become eccentrically displaced dorsally (Figure 4B). It now lay as an irregular mass of neurons about the level of the skin, and the diameter along the transverse axis was much greater than that along the vertical axis. The underlying edematous mesenchyme was minimally colored (Hale 0;

AB 1+; CV 0; PAS 1+). The coalesced midline ganglionic body beneath this mesenchyme was irregularly shaped with a disorganized tail of ganglion cells trailing off laterally (side a). The opposite side (side b) contained only mesenchyme in the same area. Both sclerotomes were present, but the group of cells on side b, located immediately lateral to the central ganglionic mass, showed no histochemical staining. On the contralateral side, the corresponding mass was more laterally placed and likewise exhibited no histochemical staining. However, the latter group of cells were separated from the subspinal cord mesenchyme by a continuous sheet of ganglion cells. The somite on side a had moved to a more medial position, but a similar change had not occurred on the opposite side (b). The centrum lay below the central ganglionic mass in its normal position. Normal staining occurred (Hale 3+; AB 2+; CV 2; PAS 0).

In the next caudal segment (lesion level 4), the ganglia were again separate and lateral in position (Figure 4C). At this point, the somites had joined across the midline above the centrum. The centrum demonstrated diminished staining (Hale 3+; AB 2+; CV 1; PAS 0), while the mesenchyme beneath the spinal cord was minimally stained (Hale 0; AB 1; CV 0; PAS 2), as were the sclerotomic aggregates (Hale 0; AB 0; CV 0; PAS 1).

At lesion level 5, the ganglia had formed two neural bodies in the midline, and myotomic interlayers were still present (Figure 4D). (Myotomic interlayers are defined as the lateral somite of one side joined across the midline with the lateral somite of the contralateral side, forming tissue layers between the centrum and spinal cord.) The dorsally eccentric spinal cord lay over the ganglion bodies and the subspinal cord mesenchyme (Hale 1; AB 1; CV 0; PAS 0). The sclerotomes demonstrated

essentially no coloring (Hale 1; AB 0; CV 0; PAS 0). The centrum was still displaced ventrally and reduced in size.

At the anterior borders of the posterior limb buds (lesion level 6), the ventral portion of the spinal cord shifted toward a more normal position closer to the notochord (Figure 4E). The lateral portions of the opened spinal cord still remained flattened above the cutaneous dorsal surface of the fetus, and as before, there was evidence of moderate degenerative changes on the exposed surface. The ganglia had assumed their normal lateral position, and ventral to them were the stained sclerotomic cell aggregates of the future neural arches (Hale 2+; AB 2; CV 0; PAS 1+). Mesenchyme immediately ventral to the spinal cord tissue remained edematous, and the portion beneath the ventrally projecting tissue was colored Hale 1+, AB 1+, CV 0, PAS 0. The centrum was found to be in direct contact with this colored mesenchyme and demonstrated staining graded Hale 2+, AB 1+, CV 1+, PAS 0. Lateral myotomic tissue was no longer above the centrum but now lay in the normal lateral position.

At the level of the middle of the posterior limb bud (lesion level 7), the lesion was less marked (Figure 4E). The ventral portion of the spinal cord approached a normal position while the dorsal half remained as an exposed remnant laterally on the cutaneous surface. Morphology and histochemical properties were once again within the normal range except for absence of cresyl violet staining in mesenchyme and neural arches. The abnormal staining pattern demonstrated by the neural arch and subspinal cord mesenchyme in cross-sections is represented in Table VI and graph 2. The normal pattern derived from fetus N14₁-6 (Table V, graph 1), when correlated with the experimental results (Table II), demonstrated no such fluctuations in the Hale reaction, alcian blue, or cresyl violet at the reading levels II (corresponding to lesion levels

2, 3, and 4) and III (lesion level 5).

B. Fourteen-day-old fetus: E14₁₋₃. Fertilization age 14 days \pm 1 hour. Crown-rump length was unavailable. Wet weight 214.2 mgm. Cross-sectioned. The fetal tissues were well preserved throughout processing with minimal histochemical staining variability between sections. A myeloschisis deformity was noted grossly which extended from the level of the diaphragm to the caudal segments of the posterior limb buds.

A dorsal displacement of the spinal cord was first observed in the superior portions of the lesion. This gradually formed an exposed eccentric mass of flattened neural tissue on the dorsal surface of the fetus, and beneath this tissue at the midlimb bud segments, lay the ganglia and minimally stained sclerotomes. The mesenchyme beneath the spinal cord colored only in the regions approximating the original ventral portions of the spinal cord. In midlesion, the centra were reduced in size and were separated from this mesenchyme by medially displaced myotomic tissue which had formed intervening layers. Staining of mesenchyme at these midlesion levels was reduced, accompanied by minimal intercellular coloring in the sclerotomes.

At the caudal segments of the posterior limb buds, the spinal cord still remained on the dorsal surface of the fetus, but it was not as disorganized. The underlying structures were now in closer proximity to it, for the myotomes had again assumed a more lateral position. The mesenchyme beneath the cord was more prominently colored, as was the normal-appearing centrum, while each sclerotome also exhibited increased staining. Caudal to the lesion, morphology and histochemical properties were normal. The abnormal staining pattern demonstrated by the neural

arch and subspinal cord cross-sections is represented in Table VII and graph 3. The normal pattern derived from fetus N14₁₋₆ (Table V; graph 1), when correlated with the experimental results (Table II), demonstrated no such fluctuations in the Hale reaction, alcian blue, or cresyl violet at the reading levels III (lesion levels 2 and 3) and IV (lesion levels 4 and 5).

C. Fourteen-day-old fetus: E14₃₋₅. Fertilization age 14 days \pm 1 $\frac{1}{4}$ hours. Crown-rump length 0.99 cm. Wet weight 123.4 mgm. Sagittally sectioned. The tissues were well preserved throughout processing with minimal variation in histochemical staining between sections. Since this fetus was sectioned sagittally, it was chosen for description so regional variations at different lesion levels along the sagittal plane could be compared simultaneously. Microscopic examination revealed a myeloschisis deformity had developed between L 4 and Co 1.

A midline section through the lesion is represented by Figure 3C. Cartilage was not yet present in post-axial portions of this embryo. Subspinal cord mesenchymal staining cranial to the anterior portions of the lesion (lesion level 1) was easily identified (Hale 2+; AB 2+; CV 1+; PAS 1+), as were the sites of the future centra in the same region (Hale 3+; AB 3+; CV 2+; PAS 0). The pre-neural arch portions of sclerotomal aggregates in more lateral sections were also stained (Hale 2+; AB 1+; CV 0; PAS 0).

In the anterior region of the lesion, the enlarged ganglia coalesced in the midline over two vertebral segments. The overlying spinal cord was dorsally displaced and its dorsal surface was exposed to the exterior. Staining of the subspinal cord mesenchyme was minimal (Hale 0; AB 1+; CV 0; PAS 1+). The underlying future centra were

ventrally displaced and showed diminished affinity for the stain except in the ventral portions around the notochord (Hale 2+; AB 2+; CV 0; PAS 0). More lateral pre-neural arch staining was absent (Hale 0; AB 0; CV 0; PAS 0).

At the midlesion levels, the centrally coalesced ganglia and dorsally displaced cord were still as above. The subspinal cord mesenchyme remained unstained (Hale 0; AB 1+; CV 0; PAS 1+), while the centra still stained as above (Hale 2+; AB 2+; CV 0; PAS 0), but now the pre-central region stained both dorsally and ventrally. The pre-neural arch regions were unstained (Hale 0; AB 0; CV 0; PAS 0).

In the posterior portions of the lesion, the overlying deformed neural tissue and midline ganglia were noted to be still present. The subspinal cord mesenchyme remained uncolored (Hale 0; AB 1+; CV 0; PAS 1+); the centra were now in their normal position and stained prominently (Hale 3+; AB 3+; CV 1+; PAS 0); and the laterally placed, pre-neural arch tissue was minimally colored (Hale 1+; AB 0; CV 0; PAS 0).

In the region immediately caudal to the lesion, the normal morphological relationships were re-established. The subspinal cord mesenchyme was stained (Hale 2+; AB 2+; CV 1+; PAS 1+); the centra were stained (Hale 3+; AB 3+; CV 0; PAS 0); but at no level were the ganglia or spinal cord tissues stained for mucopolysaccharides.

The abnormal staining pattern demonstrated by the neural arch and subspinal cord mesenchyme in sagittal sections is represented in Table VIII and graph 4. The normal pattern derived from fetus N14₁-6 (Table V, graph 1), when correlated with the data in Table I, demonstrated no such fluctuations in the Hale reaction, alcian blue, or cresyl violet between reading levels IV (corresponding to lesion levels 2 and 3) and V (lesion level 4).

D. Fifteen-day-old fetus: E15₆-11. Fertilization age 15 days + 1 hour. Crown-rump length 1.18 cm. Weight 194.0 mgm. Cross-sectioned. The fetal tissues were well preserved throughout processing with minimal histochemical staining variability between sections. A myeloschisis deformity was noted grossly which extended from the levels located at the anterior portion of the posterior limb buds to the segments located immediately caudal to the posterior limb buds.

At the level just superior to the posterior limb buds (through the kidneys), the lesion was not yet apparent. The only deviation from normal was a slight increase in the transverse diameter of the cord. The remaining structures were within the limits of normal.

Within a few caudal segments (lesion level 1), the spinal cord became elevated dorsally but remained covered by skin (Figure 5A). The sclerotomic cell flow dorsal to the cord was indistinguishable from the overlying skin. In the edematous mesenchyme ventrolateral to the spinal cord, marked staining occurred (Hale 3+; AB 3+; CV 2+; PAS 1+ near cord and 2+ near centrum). The centrum immediately below this mesenchyme was altered in position and form. Though the notochord remained in the normal position and the surrounding cartilage was well stained (Hale 4+; AB 4+; CV 3+; PAS 2+), there had occurred a dorsal extension of this cartilage mass toward the mesenchyme beneath the elevated spinal cord. This protraction was occupied by two areas of intercellular staining (Hale 4+; AB 4+; CV 3+; PAS 2+) which were continuous laterally with extensions toward the early neural arches. The neural arches were easily recognized as areas of good intercellular staining (Hale 3+; AB 3+; CV 3+; PAS 1+) located lateral to the normally placed ganglia. The lateral somites remained in their normal positions.

At the level of the middle of the limb bud (lesion level 2),

the spinal cord became a little more dorsally displaced, but the overlying cutaneous structures were still intact (Figure 5B). The mesenchyme ventral to the cord exhibited decreased staining (Hale 1+; AB 1+; CV 0; PAS 1+). The ganglia had moved to a more ventrolateral position and were increased in size, forming an interrupted layer between the mesenchyme and the structures below. Immediately ventral to the spinal cord, myotomic cell layers had formed intervening sheets over the normally placed, but smaller, centrum. The centrum matrix had stained less than normally (Hale 2+; AB 2+; CV 2+; PAS 0), and the neural arch sclerotome evidenced minimal staining of matrix (Hale 1+; AB 1+; CV 0; PAS 3+).

At the caudal level of the posterior limb buds (lesion level 3), the dorsally eccentric spinal cord had increased along the dorso-ventral axis while narrowing along the transverse axis (Figure 5C). The entire structure was tilted to one side with a depression evident on the dorso-lateral (side a) surface of the embryo. Below the cord a single, midline, coalesced, ganglionic mass occurred. Minimal mesenchyme was present between the cord and this structure, and no staining was evident in this mesenchyme. In the depressed area noted above, a small mass of neural tissue lay above the skin layer; below this (lateral to the spinal cord and fused ganglia below it) was a small mass of ganglionic cells. There was minimal staining in the surrounding sclerotomes (Hale 0; AB 1+; CV 0; PAS 3+). The myotomic cell layers were present as above, continuing to separate the ganglion accumulations from the centrum below. The centrum colored prominently (Hale 3+; AB 3+; CV 2+; PAS 0) but was reduced in size from normal.

Within two segments (lesion level 5D), the spinal cord as seen before had disappeared. Replacing it was a very dorsally-arched,

eccentric mass of neural tissue (Figure 22). No epithelium covered this structure on its dorsal surface, and there was evidence of moderate degenerative change. Below the cord was the minimally stained mesenchyme (Hale 0; AB 2+; CV 0; PAS 1); underlying the mesenchyme was a large, midline, ganglionic mass; and ventrolateral to this were the neural arch sclerotomic masses (Hale 2+; AB 2+; CV 1+; PAS 2+). The underlying centrum was easily recognizable (Hale 4+; AB 3+; CV 3+; PAS 1+). The lateral somitic tissue had again regained its normal position. However, this section was in the rump of the animal, and since this was a partial frontal section, the vertebral and sclerotomic structures actually corresponded to the spinal cord's morphology and its underlying unstained mesenchyme located a half-segment more posteriorly.

In the rump curve (lesion level 5), depicted in Figure 5E, the neural arch sclerotomes assumed prominent staining (Hale 2+; AB 2+; CV 1+; PAS 1+) as did the centrum (Hale 3+; AB 3+; CV 2+; PAS 0) and the ventral spinal cord mesenchyme (Hale 1+; AB 3+; CV 1+; PAS 0). In the distal rump curve, the lesion disappeared so that normal morphology and histochemical properties could be observed.

The abnormal staining pattern demonstrated by the neural arch and subspinal cord mesenchyme cross-sections is represented in Table IX and graph 6. The normal pattern derived from fetus N15₄-6 (Table IV, graph 5), when correlated with the experimental results (Table II), demonstrated no such fluctuations in the Hale reaction, alcian blue, or cresyl violet at the reading levels III (corresponding to lesion level 2), IV (lesion level 3), and V (lesion level 4).

E. Fifteen-day-old fetus: E15₇-11. Fertilization age 15 days \pm 1 hour. Crown-rump length 1.30 cm. Wet weight 232.4 mgm. Cross-

sectioned. The fetal tissues were well preserved throughout processing with minimal histochemical staining variability between sections. A myeloschisis was noted grossly which (not unlike that in the previous fetus) extended from superior segments of the posterior limb buds to the caudal levels of the posterior limb buds.

A medial migration of the ganglia and lateral somitic tissue toward the midline followed the initial dorsal elevation of the spinal cord. Myotomic cell interlayers were then formed, and the overlying ganglia were found to coalesce intermittently in the midline. Included with the midline structures were randomly distributed nerves, smaller ganglionic masses, and loose mesenchymatous tissues. Corresponding to these deviations, there was a diminishment in the subspinal cord mesenchyme staining, and in one segment coloring was completely absent. Concurrently, at these anterior and midlesion levels, the neural arches had migrated to a more ventromedial position beneath the deformed cord where they remained in direct continuity with a dorsal extension of the ventrally displaced centrum. Soon this articulation disappeared, and the neural arches were represented by minimal intercellular staining of the sclerotomic aggregates. These aggregates either lay ventral to the ganglia or were in direct contact with the subspinal cord mesenchyme. In one segment they were completely unstained, but this did not correspond to the more superior level at which the subspinal cord mesenchyme remained unstained. The centra were decreased in area and appeared to surround the notochord in an appositional manner with little deviation from the normal staining pattern.

In the posterior portions of the lesion, the deformed spinal cord was found to have remained in its dorsally eccentric position, but

as the ganglia, somites, and now-cartilaginous neural arches gradually assumed the normal lateral positions, the spinal cord began to shift ventrally to assume its normal position in more caudal segments. The underlying mesenchyme was unstained, and it was in direct continuity ventrally with the normal-appearing centrum. Caudal to the posterior aspects of the lesion, morphology and histochemical properties were normal.

The abnormal staining pattern demonstrated by the neural arch and subspinal cord mesenchyme cross-sections is represented in Table X and graph 7. The normal pattern derived from fetus N15₄-6 (Table IV, graph 5), when correlated with the experimental results (Table II), demonstrated no such fluctuations in the Hale reaction, alcian blue, or cresyl violet at the reading levels III (corresponding to lesion level 2) and IV (lesion levels 3 and 4).

F. Fifteen-day-old fetus: E15₆-5. Fertilization age 15 days $\pm 1\frac{1}{2}$ hours. Crown-rump length 1.32 cm. Wet weight 223.8 mgm. Sagittally-sectioned. The tissues were well preserved throughout processing with minimal histochemical staining variability between sections. Because of the plane of section, this fetus was chosen for description so the regional variations at different lesion levels could be compared simultaneously. Myeloschisis was observed grossly, and microscopic examination revealed the deformity had developed between L 1 and S 3.

Just anterior to the deformity (lesion level 1), subspinal cord mesenchyme staining was observed (Hale 2+; AB 2+; CV 1+; PAS 1+). The centra were in a normal position and stained within normal limits (Hale 4+; AB 3+; CV 3+; PAS 1+). The neural arches were likewise normal in position and staining (Hale 4+; AB 3+; CV 2+; PAS 1+).

At the anterior portions (lesion level 2) of the lesion which extended from L 1 to L 3, a midline ganglionic mass and myotomic interlayers appeared, but no cord defect was yet observable. There was a slight ventral displacement (Hale 3+; AB 2+; CV 1+; PAS 1+) of the centra and accompanying notochord, and the subspinal cord mesenchyme (Figure 3D) demonstrated diminished staining (Hale 0; AB 0; CV 0; PAS 1+), as did the neural arches (Hale 0; AB 0; CV 0; PAS 1+).

The initial abnormality seen in the spinal cord occurred between L 3 and L 5 (lesion level 3) and consisted of a dorsally displaced, denuded, neural tissue mass. The midline ganglionic masses were intermittently present, and the myotomic interlayers still extended across the midline. The centra and accompanying notochord were displaced further ventrally with staining now only in the ventral portions of the centrum in the area surrounding the notochord (Hale 3+; AB 2+; CV 1+; PAS 1+). The subspinal cord mesenchyme remained minimally stained (Hale 0; AB 0; CV 0; PAS 1+) as did the neural arches (Hale 1+; AB 1+; CV 0; PAS 1+).

In the posterior half of the lesion between L 5 and S 2, the spinal cord remained eccentric and denuded dorsally. The sporadic ganglionic masses and myotomic interlayers were still in the midline (Hale 3+; AB 2+; CV 2+; PAS 1+). The centra and notochord were ventrally displaced, and the subspinal cord mesenchyme was stained (Hale 0; AB 1+; CV 0; PAS 1+). Normal staining was demonstrated by the neural arches (Hale 2+; AB 2+; CV 1+; PAS 1+).

At S 2 and S 3, normal morphological relationships were re-established (lesion level 5). The centra were stained normally (Hale 4+; AB 2+; CV 2+; PAS 1+) as were the neural arches (Hale 2+; AB 2+; CV 1+;

PAS 1+) and the subspinal cord mesenchymal elements (Hale 2+; AB 2+; CV 1+; PAS 1+). At no level was the spinal cord or ganglionic tissue observed to stain for mucopolysaccharides.

The abnormal staining pattern demonstrated by the neural arch and subspinal cord mesenchyme in sagittal sections is represented in Table XI and graph 8. The normal pattern derived from fetus N15₄-6 (Table IV, graph 5), when correlated with the experimental results (Table II), demonstrated no such fluctuations in the Hale reaction, alcian blue, or cresyl violet at the reading levels III (corresponding to lesion levels 2 and 3) and IV (lesion level 4).

G. Sixteen-day-old fetus: E16₄-5. Fertilization age 16 days \pm 1 hour. Crown-rump length 1.38 cm. Weight 325.6 mgm. Cross-sectioned. The fetal tissues were well preserved throughout processing with minimal histochemical staining variability between sections. Gross observation demonstrated that a myeloschisis deformity had developed, and subsequent microscopic examination showed the deformity to extend from the segments immediately anterior to the posterior limb buds to the caudal levels of the posterior limb buds.

At the mid-renal level (lesion level 1) superior to the posterior limb buds, the dimensions of the slightly dorsally-elevated spinal cord became altered such that the diameter along the transverse axis was increased while the vertical axis was decreased (Figure 6A). The cell flow from the lateral sclerotomes and the overlying skin was present but disrupted by artifacts. The mesenchyme approximating the ventral and ventrolateral aspects of the spinal cord was stained (Hale 2+; AB 2+; CV 1+; PAS 2, ventral portion). Lateral to the spinal cord, the ganglia appeared in their normal positions; lateral and ventral to these ganglia

were the definitive neural arch cartilage bodies, which on one side projected in a dorsal extension on the normally placed centrum. Both this extension and the neural arches were stained (Hale 4+; AB 4; CV 4+; PAS 1+). The centrum itself was reduced in size but showed no diminished staining (Hale 4; AB 4+; CV 4+; PAS 3+). The lateral scimites were in their normal positions.

Slightly posterior (lesion level 2), the intact spinal cord continued to increase in diameter along the horizontal axis while decreasing along the vertical axis (Figure 1B). The skin and sclerotomic cell flow dorsal to the cord were intact. The ganglia had coalesced beneath the cord with two small ganglionic bodies still remaining along the ventrolateral surface of the cord. The ganglionic mass on side a approximated the central ganglionic mass, whereas a broad gap existed between this central mass and the small one on side b. The gap was filled by unstained mesenchyme which was continuous with mesenchyme ventral to the spinal cord (Hale 1+; AB 1+; CV 0; PAS 2+, ventral portion). Beneath the gap stood the sclerotome of side b, which was colored (Hale 1+; AB 1+; CV 0; PAS 2+). On the contralateral side, the sclerotome was separated from the mesenchyme ventral to the spinal cord by the ganglionic mass, and it remained unstained (Hale 0; AB 1+; CV 0; PAS 3+). The lateral myotomes had migrated medially and joined with each other across the midline to form myotomic interlayers under the central ganglionic mass. The underlying centrum was reduced in size as compared to normal and had stained (Hale 4+; AB 4+; CV 4+; PAS 2+). The notochord remained normal in appearance and location.

Within the next few caudal segments (lesion level 3), the small lateral ganglionic masses disappeared and the neural arch sclerotomic tissue were blended with the myotomic interlayers that were more prominent

with PAS 3+ interstitial staining (Figure 1C). There presented a smaller midline mass above which edematous subspinal cord mesenchyme colored minimally in the midline (Hale 1+; AB 1+; CV 0; PAS 1+ in the lateral portions).

Caudal to this region at the superior level of the posterior limb buds (lesion level 4), the spinal cord remained dorsally exposed and open (Figure 6D). The centrum was within normal limits in size, and staining was variable (Hale 4+; AB 4+; CV 4+; PAS 2+). The structures dorsal to the cord had not persisted (cell flow and skin), and minimal degenerative changes of the spinal cord took place on its external surface.

At the cranial level of the posterior limb buds, the dorsally eccentric spinal cord was soon accompanied ventrolaterally (Figure 1E) by two large aggregates of spinal cord tissues derived from it (lesion level 5). No cutaneous covering protected these structures dorsally. Ventral to these spinal cord tissues, the edematous mesenchyme stood unstained, except in a small area immediately beneath the midline, ventral to the spinal cord (Hale 0; AB 1; CV 0; PAS 1+). No staining occurred beneath the new, laterally placed, spinal cord tissue. Two circular cartilage bodies, presumably neural arches (Hale 4+; AB 4+; CV 4+; PAS 2+), were seen in the somitic interlayers beneath this mesenchyme (which was derived from a dorsal extension of the centrum. The dorsal edge of the myotomic interlayer stained (Hale 1+; AB 2+; CV 0; PAS 4+), but the normally positioned, but still smaller than normal, centrum was well colored (Hale 4+; AB 4+; CV 4+; PAS 2+).

At the mid-posterior limb bud level (lesion level 6), the two lateral spinal cord tissue masses had coalesced to form one large cap over the dorsal surface of the fetus (Figure 6F). The underlying

edematous mesenchyme stained (Hale 2; AB 2+; CV 1; PAS 2+). There was one discrete ganglion body on each side of the midline dorsolateral to the centrum (Hale 4+; AB 4+; CV 4; PAS 3+). Ventral to these ganglionic bodies, short processes extended from the midline centrum (Hale 4+; AB 4+; CV 4; PAS 2+). The lateral somites were present in their normal position.

At the posterior limb bud level (lesion level 7), the subspinal cord mesenchyme showed staining (Hale 1+; AB 2+; CV 1+; PAS 2+). The normal sized centrum (Hale 4; AB 4; CV 3; PAS 2) and short neural arch processes (Hale 4; AB 4; CV 2; PAS 2) were present as above.

Caudal to the limb buds in the rump curve, morphology and histochemical properties returned to normal.

The abnormal staining pattern demonstrated by the neural arches and subspinal cord mesenchyme cross-sections is represented in Table XII and graph 10. The normal pattern derived from fetus N16₁-2 (Table V, graph 9), when correlated with the experimental results (Table II), demonstrated no such fluctuations in the Hale reaction, alcian blue, or cresyl violet at the reading levels III (corresponding to lesion levels 1 and 2) and IV (lesion levels 4 and 5).

H. Sixteen-day-old fetus: E16₄-2. Fertilization age 16 days \pm 1 hour. Crown-rump length 1.40 cm. Wet weight 333.8 mgm. Cross-sectioned. The fetal tissues were well preserved throughout processing with minimal histochemical staining variability between sections. A myeloschisis deformity was noted grossly which, upon microscopic examination, was seen to extend from the levels just anterior to the posterior limb buds to segments in the mid-portions of the posterior limb buds.

Again a slight dorsal elevation of the spinal cord with underlying edematous mesenchyme heralded the anterior portions of the lesion.

Then the spinal cord opened dorsally and flattened on the dorsal surface of the embryo. Concurrently, the ganglia and neural arches were divergent laterally, in that the arches connected to a dorsal extension of a ventrally displaced centrum. The subspinal cord mesenchyme was stained only beneath the previously ventral portions of the now flattened spinal cord. Deviations from normal varied as the lesion was studied at successively caudal levels, but, in summation (Figure 3B), the ganglia and myotomes formed intervening midline layers beneath the dorsally eccentric spinal cord. The isolated centrum ventral to these layers was decreased in size, but staining remained relatively normal. The neural arches decreased in staining, and the resultant sclerotomic masses varied in position from midline to more lateral sites. These neural arch changes were seen at the same anterior and mid-lesion levels where decreased coloring of subspinal cord mesenchyme occurred.

At more posterior levels of the lesion, the altered morphology persisted, but gradually the flattened spinal cord moved ventrally with the ganglia, myotomes, and neural arches (Hale 2+; AB 1+; CV 0; PAS 3+), assuming more lateral positions. The centra were unaltered in size and histochemical reactions, and the subspinal cord mesenchyme still stained less intensely than normal. Finally, at the mid-posterior limb bud levels, the normal morphology and histochemical properties of these tissues were restored.

The abnormal staining pattern demonstrated by the neural arches and subspinal cord mesenchyme cross-sections is represented in Table XIII and graph 11. The normal pattern derived from fetus N16₁-2 (Table V, graph 9), when correlated with the normal experimental results (Table II), demonstrated no such fluctuations in the Hale reaction, alcian blue, or cresyl violet at the reading level II (corresponding to lesion levels 3 & 4).

Discussion

The normal centrum and neural arch development in the posterior axial skeleton exhibited a definite pattern of acidic mucopolysaccharide production in the cartilage matrix. This development was divided into three phases, according to the distribution of the acidic mucopolysaccharides: 1) precartilaginous, 2) cartilaginous, and 3) preosseous.

The first indication that the centrum and neural arch matrix were present occurred in the 13-day-old fetuses. There was a minimal staining of fine, fiber-like structures between the cells in the sclerotic aggregates. By the fourteenth day staining was more prominent, with some color occurring between the small, fiber-like structures; but no definitive cartilage was yet present in the posterior axial regions. Then, in the 15-day-old fetuses at the level of the posterior limb buds, the centra and neural arches morphologically differentiated into cartilage. This rapid transition had taken place at some time during the twenty-four hour period between the fourteenth and fifteenth days, and in the rump of a 15-day-old fetus, a region of sharp transition from precartilage to definitive cartilage extended over a distance of four to five segments. The new cartilage matrix assumed a different histochemical pattern and entered the cartilaginous phase of acidic mucopolysaccharide staining, (Figure 3A).

This second phase of matrix staining was marked by two distinct staining patterns. The first was represented by the Hale reaction. On the fifteenth day, the matrix initially assumed an irregular pattern of bundle-like structures accompanied by more widely distributed, granule-like material (Figure 1A). During the next three days, there was a gradual redistribution of the intercellular materials, so that by the

seventeenth and eighteenth days (Figure 2A) only a strongly stained, granular-appearing material remained around the lacunar spaces. The remainder of the homogeneous-appearing matrix stained less intensely. During the sixteenth, seventeenth, and eighteenth days, a different pattern was present in the region of the future ossification centers, ventral to the neural arch region just described as the cartilaginous phase. In the preosseous matrix, the deeply stained, band-like appearance of the matrix was prominent, but the amount of matrix markedly diminished. The lacunar spaces enlarged but contained only atrophic small cells. The second staining pattern in the cartilaginous phase of matrix histochemistry showed a different distribution of acidic mucopolysaccharides as demonstrated by the alcian blue and cresyl violet staining reactions. With these techniques, the matrix did not contain any granular-appearing material, and with aging, the perilacunar distribution of intensely stained material was not observed. From the fifteenth (Figure 1B) through the eighteenth days (Figure 2B), the fine, fiber-like material of the matrix developed into prominently stained bundles coursing in the matrix between the lacunae. In the regions where preosseous changes were occurring, there was accentuation of the bundle-staining, but the matrix again reduced in extent, secondary to the lacunar space expansion. The cresyl violet pattern in phases two and three (Figures 1C and 2C) did not differ from that of alcian blue. However, the cresyl violet metachromasia was more specifically limited to the cartilage matrix, in contrast to the Hale reaction and the less specific alcian blue stain.

The study of normal neural arch and centrum development demonstrated four points. First, there were three stages of histochemical morphology defined: 1) precartilaginous, 2) cartilaginous, and 3) pre-

osseous. Secondly, the transition of the precartilaginous elements to definitive cartilage occurred rapidly, and along the sagittal axis the transition zone was correspondingly short (four to five segments). Finally, in the cartilaginous phase two different histochemical patterns of acidic mucopolysaccharides were demonstrated in the matrix of centra and neural arches. This is an interesting point, for the presence of two different patterns of acidic mucopolysaccharides could be interpreted several different ways. First, one may assume that one of the patterns is artefactual and inherent in the histochemical method, the techniques and stains being different for both patterns. Secondly, the three reactions might vary in sensitivity (wider distribution), though this is an unlikely explanation since the least sensitive (alcian blue) and the most sensitive (cresyl violet) methods stain with a similar pattern. The Hale reaction, representing an intermediate sensitivity, reacts unlike either of these. Finally, two different acidic mucopolysaccharides may be present, one being stained by the Hale, and possibly alcian blue and cresyl violet, and the other only by the alcian blue and cresyl violet stains. There is no experimental evidence that such a separation of mucopolysaccharides exists.

The PAS-positive substances did not seem to play a prominent role in chondrogenesis. On the thirteenth and fourteenth days, PAS-positive material occurred intercellularly in the neural arch sclerotomes, and it developed at sites where acidic mucopolysaccharides would soon be stained. Other than during this phase of precartilage development, the positive reactions were very minimal in the cartilaginous matrix (Figures 1D and 2D). However, staining was present in the cytoplasm of the cartilaginous and preosseous cells (Figure 2D). PAS-staining was prominent in tissues other than cartilage, such as somites, subspinal cord

mesenchyme (the ventral portion where meninges would develop) and the cutaneous layers. In essence, though the PAS-positive material was detected in precartilaginous and cartilaginous structures and in other tissues, no implications for chondrogenesis were drawn from their appearance.

The normal notochord, previously implicated in appositional cartilage development of the centra (125,32), demonstrated interesting histochemical properties. In all fetuses the acellular perinotochordal region stained intensely with the acidic mucopolysaccharide procedures. This coloring was distinct from the less intense matrix-staining in centra of earlier animals which had no well defined cartilage (13- and 14-day-old). In the older fetuses with definitive cartilaginous centra (16-, 17-, and 18-day-old) this perinotochordal staining blended with the matrix. In previous investigations (25) a substance capable of inducing cartilage in somite cultures has been extracted from the notochords of chicks. This inducing agent cannot be distinguished chromatographically from a similar inductive extract of the ventral portions of the spinal cord in chicks. The relationship between the perinotochordal staining and the inductive activity of the notochord may be related to the process of appositional cartilage formation.

The central notochord also demonstrated a core of acellular, homogeneous material that stained only with the alcian blue (Figure 3A) and cresyl violet techniques. In younger fetuses (14- and 15-day-old), the stained material appeared to represent a cylindrical rod running longitudinally within the notochord. In the older fetuses (16-, 17-, and 18-day-old), progressive development of intervertebral enlargements (beading) and intracentrum degeneration of the notochord occurred. Concurrently, the distinct central core disappeared in the intracentrum

portions or was represented there by randomly distributed intercellular spots. In summary, the histochemical reactions of alcian blue and cresyl violet in the normal central and perinotochordal regions paralleled the histochemical properties demonstrated in the normal cartilage matrix. Once again the Hale reaction behaved unlike the other two techniques, both in the irregular nature of the perinotochordal staining and in the absence of the central core staining. Whether this was secondary to a difference in techniques or due to real differences (i.e., two acidic mucopolysaccharide components) is unknown.

In the normal animals, the mesenchyme located between the spinal cord and the surrounding centrum and neural arches (Figures 1A, 1B, and 1C) was stained by all three techniques demonstrating the acidic mucopolysaccharides. This staining was limited to the subspinal cord mesenchyme below the level at which the dorsal spinal roots entered the cord. This distribution is correlated with the findings of previous investigators who have demonstrated the importance of the ventral spinal cord in chondrogenic induction (15,31,32,33). The subspinal cord mesenchyme is located in a position which the inducer elaborated by the ventral portions of the spinal cord must pass to reach its target. From this finding it is concluded that the histogenic inductive material found mesodermally-derived cells receptive to its influence. Because these cells are not as well differentiated as the sclerotomal elements, they do not respond by forming cartilaginous elements, but develop, instead, histochemical properties similar to very early 13-day-old cartilage matrix (i.e., secretion of small amounts of acidic mucopolysaccharides). If such a mechanism is operating to induce these histochemical properties, any alteration in the elaboration of the inductive material should result in a corresponding change in staining of the sub-

spinal mesenchyme. As has been discussed earlier, a relationship between this histogenic inductive mechanism and chondrogenesis has been experimentally defined. Therefore, a relationship between the histogenic inductive mechanism, the subspinal cord mesenchyme, and the neural arches may be postulated if both the neural arch and subspinal cord mesenchyme show parallel histochemical changes in response to a deformed spinal cord (i.e., an altered histogenic inductive mechanism -- see Introduction).

The experimental studies revealed several points of interest. First, deviations were present in centrum development at the region of the lesions. Results of in vitro studies (32) with chick somite and spinal cord cultures appear to be related to the alterations noted in myeloschisis. The in vitro study demonstrated that placement of an intervening milipore filter between spinal cord and early somitic tissue delayed the development of cartilage bodies in the somite tissue. In the myeloschisis lesions, myotomic and ganglionic tissues were seen to cross the midline in some specimens, thereby placing an in vivo barrier between the spinal cord tissue and the cartilage below. Some animals with this morphology responded by producing minimal cartilage in the centra (Figures 3B and 3C). This appeared to surround and conform to the circular structure of the notochord, giving the cartilage the appearance of appositional structure. No decrease in the staining properties of the formed cartilages occurred with any consistency. Such changes were present, however, in a few instances where the absence of subspinal cord mesenchyme staining was the only other alteration present. Another factor which possibly contributed to altered centra development was the increased distance separating the spinal cord and these structures. This was noted to be secondary to ventral displacement of the centra and notochord and dorsal displacement of neural tissue (Figure 3C).

This increased the distance across which a histogenic inductive agent had to be effective.

Of the several marked alterations accompanying the myeloschisis lesions, most prominent was the decrease in acidic mucopolysaccharide-staining in the neural arch matrix ventrolateral to the deformed neural tissue (Figure 3B). The change was either a total absence of staining or a decrease in staining. In comparing the normal and deformed fetuses, it was concluded that these changes represented states of immaturity or retardation rather than agenesis. This was felt to be the case because of the presence, in some animals, of minimal staining in the most severely affected regions of the lesion. However, at the present time, no conclusive evidence can be presented which supports this concept of immaturity or retardation versus agenesis.

Frequently accompanying the myeloschisis lesions was absent or diminished staining of the subspinal cord mesenchyme (Figures 3B, 3C, and 3D). The ten cases presented in the results demonstrate that simultaneous alterations occurred in both of the neural arches beneath portions of the lesions. These changes are represented in the tables and in graphs 2, 3, 4, 6, 7, 8, 10, and 11 which demonstrate the occurrence of a consistent pattern in each lesion. In these graphs staining of neural arch and subspinal cord mesenchyme are plotted from values recorded for each at the same levels. The pattern demonstrated in each lesion is a diminution in the staining of both structures at the same levels. This change predominantly occurred in the anterior half of each lesion. It seems certain that these concomitant decreases in staining of subspinal cord mesenchyme and neural arch matrix are more than chance and may represent an important observation. The findings of other investigators presented in the introduction, the results in the present study of normal

fetuses, and the presumptive evidence from the experimental data indicate the probability that a causal relationship exists between the deformed spinal cord and the altered histochemical properties seen in the sub-spinal cord mesenchyme and neural arch matrix. This relationship is presumed to occur through an alteration in the inductive mechanism mediated by the ventral spinal cord. However, the hypothesis advanced in the introduction is not completely substantiated. To reiterate, I proposed that an alteration in the histogenic inductive system may lead to altered acid mucopolysaccharide elaboration during chondrogenesis. Although the evidence presented in this study is only presumptive, (since no direct evaluation of the histogenic inductive mechanism has been made), such inferences as have been made seem reasonable in the light of the alterations described above.

In order to verify the original hypothesis, a further work would be necessary. To evaluate better the histogenic inductive mechanism, I would suggest the use of tissue culture technique. Early normal somites from rat fetuses would be cultured, and the deformed portions of spinal cords from trypan blue-induced myeloschisis would be explanted to the cultures. The number and character of cartilage nodules formed would then be tabulated and statistically compared with a normal study. Both would be statistically tested against the cartilage developed in somite cultures without transplants. In this manner the histogenic inductive capacity of the deformed spinal cords could be ascertained. If more conclusive information were desired, extracts from deformed spinal cords could be made and their histogenic inductive capacities tested in somite cultures.

The possibility of diminished receptivity of the cells in both the mesenchyme and sclerotomes could of course account for the changes

that occur without an alteration in the histogenic inductive mechanism. Such an alteration could be considered secondary to the lesion or to the direct action of trypan blue. If the latter is accepted as a possibility, future deformities could be produced by other means (54) and the study repeated to determine if the alterations persist or become markedly changed.

Summary and Conclusions

1. The normal developmental pattern of acidic mucopolysaccharides in the matrix of the neural arches and centra of the posterior axial skeleton has been divided into three stages in terms of histochemical morphology: 1) precartilaginous, 2) cartilaginous, and 3) preosseous.
2. The transition from the precartilaginous to the cartilaginous matrix for any one vertebral level was a rapid process, and the regions exhibiting this change extended over four or five vertebral levels.
3. In the cartilaginous phase, two acidic mucopolysaccharide patterns were present in the matrix of the neural arches and centra. Whether this discrimination was secondary to artifacts of stain technique or actually representative of two separate mucopolysaccharide fractions in the developing cartilage is unknown.
4. Centra development from the precartilaginous to the cartilaginous state was approximately two to three vertebral levels ahead of the corresponding changes seen in the neural arches.
5. In the fetuses with myeloschisis, the centra ventral to the lesions demonstrated reduction in size with little consistent alteration of acidic mucopolysaccharide staining. In some specimens the smaller cartilage mass assumed the circular form of the enclosed notochord. Accompanying this change were variable combinations of the following abnormalities: absence of the subspinal cord mesenchyme staining; intervening myotomic and ganglionic layers between the spinal cord and centrum; and an increased distance between the spinal cord and centrum secondary to dorsal displacement of the spinal cord and

ventral displacement of the notochord.

6. The acellular perinotochordal region was rich in acidic mucopolysaccharide material. A correlation between the histogenic inductive property of the notochord, the formation of appositional cartilage, and perinotochordal staining was suggested. Observations suggesting such a process were observed in several experimental fetuses.
7. An acellular core located in the central notochord extended throughout the length of the posterior axial skeleton in 14- and 15-day-old fetuses. The histochemical reactivity of this central core was limited to alcian blue and cresyl violet stains, while the Hale reaction did not demonstrate the structure.
8. Staining occurred in the mesenchyme surrounding the ventral portions of the spinal cord. This was postulated as being a result of the inductive influence of the ventral portion of the spinal cord acting on receptive mesenchymal cells and was considered to be a coincidental change occurring at the time that the histogenic influence acted across this tissue on the sclerotomal elements.
9. At variable sites in the myeloschisis lesions, the subspinal cord mesenchyme was unstained. The predominant region of the change was in the anterior and middle portions of the defects.
10. In portions of the myeloschisis lesions, the neural arches were found to be retarded or absent and represented by their precartilage elements, the sclerotomes.
11. A correlation was established between the diminution or absence of staining in subspinal cord mesenchyme and in neural arch matrix at the same levels of the lesions.
12. The original hypothesis was not entirely verified, but the presumptive evidence indicated that a histogenic induction defect is probable in

the development of spina bifida associated with myeloschisis. A future study to evaluate directly this histogenic inductive mechanism was suggested.

References

1. Avery, G., Chow, M., & Holtzer, H. Comparison of the salamander and chick notochords in the differentiation of somitic tissues. *Anat. Rec.*, 1955. 122, 444.
2. Baldwin, W. M. The artificial production of spina bifida by means of ultraviolet rays. *Anat. Rec.*, 1915. 9, 346-356.
3. Braden, A. H. The reactions of isolated mucopolysaccharides to several histochemical tests. *Stain Technology*, 1955. 30, 19.
4. Cameron, A. H. Spinal cord lesion in spina bifida cystica. *Lancet*, 1956. 2, 171.
5. Detwiler, S. R., & Holtzer, H. The developmental dependence of the vertebral column upon the spinal cord in the urodele. *J. Exp. Zool.*, 1956. 132, 299.
6. Evans, E. E., & Mehl, J. W. Qualitative analysis of capsular polysaccharides from cryptococcus neoformans by filter paper chromatography. *Science*, 1951. 114, 10.
7. Fowler, I. Responses of chick neural tube in mechanically produced spina bifida. *J. Exp. Zool.*, 1953. 123, 115.
8. Gardner, W. J. Anatomic anomalies common to myelomeningocele of infancy and syringomyelia of adulthood suggest common origin. *Cleveland Clin. Quart.*, 1959. 26, 118.
9. Gardner, W. J. Myelomeningocele, the result of rupture of the embryonic neural tube. *Cleveland Clin. Quart.*, 1960. 27, 88-100.
10. Gardner, W. J. Rupture of the neural tube. *AMA Arch. Neur.*, 1961. 4, 1-7.
11. Gillman, J., Gilbert, C., Gillman, T., & Spence, I. Spina bifida, hydrocephalus, cleft palate, cyclophthalmia, ear defects, short tails, kinky tails, and absence of tails. *S. Afr. J. Med. Sci.*, 1948. 13, 47.
12. Gillman, J., Gilbert, C., Spence, I., & Gillman, T. A further report on congenital anomalies in the rat produced by trypan blue. *S. Afr. J. Med. Sci.*, 1951. 16, 125-135.
13. Glegg, R. E., Eidinger, D., & LeBlond, C. P. Some carbohydrate components of reticular fibers. *Science*, 1953. 118, 614.
14. Grobstein, C., & Holtzer, H. In vitro studies of cartilage induction in mouse somite mesoderm. *J. Exp. Zool.*, 1955. 128, 333.
15. Grobstein, C., & Parker, O. In vitro induction of cartilage in mouse somite mesoderm by embryonic spinal cord. *Proc. Soc. Exp. Med.*, 1954. 85, 477.

16. Gunberg, D. L. The effect of suboptimal protein diets on the teratogenic properties of trypan blue administered to pregnant rats. *Anat. Rec.*, 1955. 121, 398.
17. Haddock, N. H. Alcian blue, a new phthalocyanin dyestuff. *Research (London)*, 1948. 1, 685.
18. Hale, C. W. Histochemical demonstration of acid polysaccharides in animal tissues. *Nature*, 1946. 157, 802.
19. Hamburgh, M. Malformations in mouse embryos induced by trypan blue. *Nature*, 1952. 169, 27.
20. Holtzer, H. Experimental analysis of development of the spinal column. Part I. Response of precartilage to size variation of spinal cord. *J. Exp. Zool.*, 1952. 121, 121.
21. Holtzer, H., & Detwiler, S. R. An experimental analysis of the development of the spinal column. III Induction of skeletogenous cells. *J. Exp. Zool.*, 1953. 123, 335.
22. Holtzer, H., & Detwiler, S. R. The dependence of somite differentiation on the neural axis. *Anat. Rec.*, 1954. 118, 390.
23. Holtzer, H., Holtzer, S., & Avery, G. An experimental analysis of the development of the spinal column. *J. Morph.*, 1955. 96, 145.
24. Holtzer, H., Lash, J., & Holtzer, S. The enhancement of somitic muscle maturation by the embryonic spinal cord. *Biol. Bull.*, 1956. 111, 303.
25. Hommes, F. A., van Leeuwen, G., & Zilliken, F. Induction of cell differentiation: II. The isolation of a chondrogenic factor from embryonic chick spinal cords and notochords. *Biochem. Biophys. Acta*, 1962. 56, 320.
26. Hooghwinkel, G. J. M., & Smits, G. The specificity of the periodic acid-Schiff technique studied by a quantitative test-tube method. *J. Histo. Cyto.*, 1957. 5, 120.
27. Hotchkiss, R. D. Microchemical reaction resulting in the staining of polysaccharide structures in fixed tissue preparations. *Arch. Biochem.*, 1948. 16, 131.
28. Immers, J. Chemical and histochemical demonstration of acid esters by acetic iron reagent. *Exp. cell Res.*, 1954. 6, 127.
29. Jackson, E. L., & Hudson, C. S. Application of the cleavage type of oxidation by periodic acid to starch and cellulose. *J. Amer. Chem. Soc.*, 1937. 59(2), 2049.
30. Keiller, V. A contribution to the anatomy of spina bifida. *Brain*, 1922. 45, 31-103.

31. Lash, J. Tissue interaction and specific metabolic responses: chondrogenic induction and differentiation. *Cytodifferentiation and macromolecular synthesis*, edited by M. Locke. New York: Academic Press, 1963. Pp. 235-260.
32. Lash, J., Holtzer, S., & Holtzer, H. An experimental analysis of the development of the spinal cord. *Exp. cell Res.*, 1957. 13, 292-303.
33. Lash, J., Hommes, F., & Zilliken, F. Induction of cell differentiation. The in vitro induction of cell cartilage with a low molecular-weight tissue component. *Biochem. Biophys. Acta*, 1962. 56, 313.
34. LeBlond, C. P., Glegg, R. E., & Bidinger, D. Presence of carbohydrates with free 1:2-glycol groups in sites stained by the periodic acid-Schiff technique. *J. Histo. Cyto.*, 1957. 5, 445.
35. Lillie, R. D., et al. Reticulum staining with Schiff reagent after oxidation by acidified sodium periodate. *J. Lab. Clin. Med.*, 1947. 32(2), 910.
36. McKanus, J. F. A. Histological demonstration of mucin after periodic acid. *Nature*, 1946. 158, 202.
37. McKanus, J. F. A., & Mowry, R. W. Effects of fixation on carbohydrate histochemistry. *J. Histo. Cyto.*, 1958. 6, 309.
38. Michaelis, A. The nature of the interaction of nucleic acids and nuclei with basic dyestuffs. *Cold Spring Harbor Symp. on Quant. Biol.*, 1947. 12, 131.
39. Morgagni, G. B. *De sedibus et causis morborum 1761*. Translated by B. Alexander. London: A. Miller and T. Cadell, 1769. Cited by (8).
40. Mowry, R. W. The special value of methods that color both acidic and vicinal hydroxyl groups in the histochemical study of mucins. With revised directions for the colloidal iron stain, the use of alcian blue 8GX and their combinations with the periodic acid-Schiff reaction. *Ann. N. Y. Acad. Sci.*, 1963. 106, 402.
41. Mowry, R. W., & Winkler, Jr., C. H. Coloration of acidic carbohydrates of bacteria and fungi in tissue section with special reference to capsules of *Cryptococcus neoformans*, pneumococci, and staphylococci. *Am. J. Pathol.*, 1956. 32, 628.
42. Müller, V. G. Über eine vereinfachung der reaktion nach Hale (1946). *Acta histochemica*, 1955-56. 2, 68. Cited by (40).
43. Patten, B. Overgrowth of the neural tube in young human embryos. *Anat. Rec.*, 1952. 113, 381.
44. Patten, B. Embryological stages in the establishing of myeloschisis with spina bifida. *Amer. J. Anat.*, 1953. 93, 365.

45. Pearse, A. G. E. *Histochemistry, theoretical and applied*. Boston: Little, Brown, and Company, 1960. pp. 228-280, 831-838.
46. Rizzoli, C. Le basi istochimiche della colorazione dei mucopolisaccaridi nei tessuti con il blu Alcian 8GN. *Boll. soc. ital. sper.*, 1955. 18, 422. Cited by (40).
47. Sheppard, S. E., & Geddes, A. L. Title not available, 1942. *Rev. Mod. Phys.* 14, 303. Cited by (45).
48. Steedman, H. F. Alcian blue 8GS: a new stain for mucins. *Quart. J. Micro. Sci.*, 1950. 91, 477.
49. Strudel, G. Consequences d'l'excision de tronçons du tube nerveux sur la morphogenèse de l'embryon de poulet et sur la différenciation de ses organes: contribution à la genèse de l'orthosympathétique. *Ann. des Sc. Nat., Zool.*, 1953. 15, 251. Cited by (57).
50. Vialli, M. Osservazioni sull' uso dell' Alcian blue 8GS nello studio dei mucopolisaccaridi. *Boll. soc. ital. biol. sper.*, 1951. 27, 597. Cited by (40).
51. von Recklinghausen, F. Untersuchungh über die spina bifida. *Unch Arch*, 1886. 105, 243 & 373. Cited by (9).
52. Wagner, B. M., & Shapiro, S. H. Application of alcian blue as a histochemical method. *Lab. Invest.*, 1957. 6, 472.
53. Warkany, J., Kalter, H., & Geiger, J. *Experimental teratology*. *Ped. Cl. N. Amer.*, 1957. Nov., 983.
54. Warkany, J., Wilson, J. G., & Geiger, J. Myeloschisis and myelomeningocele produced experimentally in the rat. *J. Comp. Neur.*, 1958. 109(1), 35-64.
55. Watterson, R. L. Neural tube extirpation in fundulus heteroclitus and resultant neural arch defects. *Biol. Bull.*, 1952. 103, 310.
56. Watterson, R. L., & Spiroff, B. E. N. Development of the glycogen body of the chick spinal cord. II. Effects of unilateral and bilateral leg bud extirpation. *Physiol. Zool.*, 1949. 22, 318.
57. Watterson, R. L., Fowler, I., & Fowler, B. Role of the neural tube and notochord in the development of the axial skeleton of the chick. *Amer. J. Anat.*, 1954. 95, 337.
58. Weed, L. H. *The development of the cerebro-spinal spaces in pig and man*. Washington, D.C.: Carnegie Institute, 1917. 116 pp., 4°. Cited by (9).
59. Weiss, P., & Amprino, R. The effect of mechanical stress on the differentiation of scleral cartilage in vitro and in the embryo. *Growth*, 1940. 4, 245.

60. Wilson, J. G. Teratogenic activity of several azo dyes chemically related to trypan blue. *Anat. Rec.*, 1955. 123, 313-333.
61. Wislocki, G. B., Bunting, H., & Dempsey, E. W. Metachromasia in mammalian tissues and its relationship to mucopolysaccharides. *Amer. J. Anat.*, 1947. 81, 1.
62. Wolff, E. Les bases de la tératogénèse expérimentale des vertébrés amniotes d'après les résultats de méthodes directes. *Arch. d'Anat. d'Hist. et d'Embryol.*, 1936. 22, 1-375. Cited by (57).

Appendix

Technical Directions for the Modified Hale Reaction Method after Mowry: (40)

A. Solutions:

1. Stock Colloidal Solution: 4.4 ml of 29% FeCl_3 solution are added to 250 ml boiling distilled water. When this solution turns dark red, it is allowed to cool. This stock colloidal iron is then dialyzed for 24 hours in three changes of distilled water of a volume 5-10X that of the iron solution. It is then filtered through Whatman No. 50 paper, and the filtrate is stored at room temperature.
2. Working solution: Distilled water, 18 volumes; glacial acetic acid, 12 volumes; stock colloidal iron, 10 volumes. Made fresh each day.
3. Acetic acid, 30 per cent.
4. Potassium ferrocyanide, 2 per cent in distilled water.
5. Hydrochloric acid, 2 per cent in distilled water.
6. Harris' hematoxylin: dissolve 5 gm hematoxylin in 50 cc. absolute and 100 gm. potassium alum in 1000 cc. distilled water, both with the aid of gentle heat. The two solutions are then mixed and brought to a boil. When boiling, the flame of the burner is extinguished and 2.5 gm. of mercuric oxide is added. The solution is then mixed well, cooled by immersion of the container in cold water, and aged 2 to 3 days before use.
7. Picric acid, 0.5 per cent in distilled water.

B. Procedure:

1. Paraffin sections are taken through xylenes and graded alcohols to water.
2. Sections are placed two hours in the working solution.
3. Rinsed in three changes of 30 per cent acetic acid, 10 minutes each.
4. Washed in running tap water for 5 minutes and then rinsed briefly in distilled water.
5. Treated for 20 minutes in a freshly prepared mixture of equal volumes of 2 per cent potassium ferrocyanide and 2 per cent hydrochloric acid.
6. Washed 5 minutes in running tap water and rinsed briefly in distilled water.
7. Stained in Harris' hematoxylin for 5 minutes.
8. Washed briefly in running tap water.
9. Placed in picric acid solution for 20 seconds.
10. Rinsed for a few seconds in running tap water.
11. Dehydrated, cleared, and mounted.

C. Results: Acidic carbohydrates are colored Prussian blue in test sections but are not colored in control sections. Nuclei are red-brown. Background and cytoplasm (including erythrocytes) are yellow.

Technical Directions for the Alcian Blue 8GX-300 Stain after Mowry: (40)

A. Solutions:

1. Aqueous acetic acid, 3 per cent, in distilled water.
2. Alcian blue 8GX-300 solution: Distilled water, 97 ml; glacial acetic acid, 3 ml; Alcian blue 8GX-300, 1.0 gm. When the dye is dissolved, it is filtered and a thymol crystal is added to prevent the formation of mold. The pH is 2.8.
3. Harris' hematoxylin as in the Hale reaction.
4. Aqueous picric acid, 1.5 per cent, in distilled water.

B. Procedure:

1. Bring the paraffin section through xylenes and graded alcohols to water.
2. Rinse in 3 per cent acetic acid for 3 minutes.
3. Stain in Alcian blue solution for 2 hours.
4. Dip in tap water and then rinse 3-5 minutes in 3 per cent acetic acid.
5. Wash in tap water for 3 minutes and dip in distilled water.
6. Stain for 5 minutes in Harris' hematoxylin.
7. Wash briefly in running tap water.
8. Stain in picric acid solution for 60 seconds.
9. Rinse momentarily in tap water.
10. Dehydrate, clear, and mount.

C. Result: Complex carbohydrates rich in free acidic groups are colored turquoise blue (all connective tissue mucins and the great majority of epithelial mucins). Nuclei are red-brown. The background and cell cytoplasm are yellow.

Technical Directions for the Cresyl Violet Stain Modified from Kramer and Windrum (45):

A. Solutions:

1. Chresylecht violet solution 0.1 per cent in distilled water acidified with acetic acid to pH 2.75.

B. Procedure:

1. Paraffin sections are taken through xylenes and graded alcohols to water (tap and then distilled).
2. Immerse for 5 minutes in acidified cresyl violet solution at 35° C.
3. Distilled water rinse.
4. Two changes of 95 per cent ethyl alcohol, 1-3 minutes each.
5. One change of absolute ethyl alcohol, 3-5 minutes each.
6. Xylol clearing.

C. Result: Acidic mucopolysaccharides color purple or magenta. Lighter degrees of metachromasia represented by pink to red. Other structures light blue.

Technical Directions for the Periodic Acid-Schiff Stain after Mowry:(40)

Solutions:

1. Periodic acid solution: distilled water, 100 ml; periodic acid, 0.5 gm.
2. Schiff's reagent: Distilled water, 192 ml; concentrated hydrochloric acid, 8 ml; sodium metabisulfite, 3.8 gm; basic fuchsin (color index no. 677), 0.5 gm. Mixture is mixed well and repeatedly well shaken. 24 hours later it is filtered through Whatman No. 50 filter paper and stored in the cold and dark. No active decolorizing carbon is used just before filtering, as directed by Mowry. My reagent consequently assumes a more amber color, but results are as wished for the staining.
3. Stock (molar) sodium bisulfite solution: sodium bisulfite, 10.4 gm; distilled water, 100 ml.
4. Sodium bisulfite rinse (M/20): stock (molar) sodium bisulfite solution, 1 volume; distilled water, 19 volumes. This solution is mixed fresh.
5. Picric acid solution, 0.5 per cent.

B. Procedure:

1. Take paraffin sections through xylenes and graded alcohols to water.
2. Oxidize for 10 minutes in periodic acid.
3. Wash in running tap water for 5 minutes and rinse in distilled water briefly.
4. Treat in Schiff's reagent for 10 minutes.
5. Rinse in three changes of M/20 sodium bisulfite for 2 minutes each.
6. Wash for 5 minutes in running tap water and briefly in distilled water.
7. Stain for 5 minutes in Harris' hematoxylin.
8. Wash briefly in tap water.
9. Stain in picric acid solution for 60 seconds.
10. Rinse briefly in running tap water.
11. Dehydrate, clear, and mount.

C. Result: mucoprotein, glycoproteins, glycogen, and neutral ~~mucopolysaccharides~~ mucopolysaccharides with their vicinal hydroxyl groups are colored magenta. Nuclei are red-brown. Erythrocytes and cytoplasm of most cells are yellow.

Table I

This table summarizes the approximate vertebral levels included in the normal reading levels and the corresponding paraxial anatomic landmarks for 14-, 15-, and 16-day-old fetuses.

Reading Levels for Normals	Paraxial Anatomic Landmarks	Approximate Range of Equivalent Vertebral Levels		
		14-day	15-day	16-day
I	Lower Diaphragm	T4-5	T9-10	T9-10
II	Segments Anterior to the Posterior Limb Buds	T6-L1	T11-L3	T11-L3
III,IV,V	Segments at the Posterior Limb Buds	L1-S4	L5-Co1	S2-Co2
VI	Segments Immediately Caudal to the Posterior Limb Buds	Posterior to S4	Posterior to Co1-Co2	Posterior to Co1-Co2

Table II

This table represents a correlation of the normal reading levels and paraxial anatomic landmarks compared with the lesion levels of the cross-sectioned 14-, 15-, and 16-day-old fetuses.

Reading Levels for Normals	Paraxial Anatomic Landmarks	Lesion Levels (Experimentals; Cross-Sectioned)					
		E142-7	E141-3	E156-11	E157-11	E164-5	E164-2
I	Lower Diaphragm	-	-	-	-	-	-
II	Segments Anterior to the Posterior Limb Buds	1,2,3,4	1	-	-	1	1,2,3,4
III	Segments at the Anterior Portion of Posterior Limb Buds	5,6	2,3	1,2	1,2	2,3	5
IV	Segments at the Middle Portion of Posterior Limb Buds	7	4,5	3	3,4,5	4,5	6
V	Segments at the Posterior Portion of Posterior Limb Buds	-	6,7	4	6	6,7	-
VI	Segments Immediately Caudal to the Posterior Limb Buds	-	-	5	-	-	-

Table III

The Hale reaction (H), alcian blue (AB), and cresyl violet (CV) staining values in the centra (C), neural arches (NA), and subspinal cord mesenchyme (M) at reading levels II, III, IV, and V in the normal 14-day-old fetus (N14₁₋₆).

<u>Reading Level</u>	<u>Staining Technique</u>	<u>C</u>	<u>NA</u>	<u>M</u>
II	H	3	2	2
	AB	2	1	2
	CV	2	0	1
III	H	3	2	2
	AB	2	1	2
	CV	2	0	1
IV	H	3	2	2
	AB	2	1	2
	CV	2	0	1
V	H	3	1	2
	AB	2	0	2
	CV	2	0	1

Table IV

The Hale reaction (H), alcian blue (AB), and cresyl violet (CV) staining values in the centra (C), neural arches (NA), and subspinal cord mesenchyme (M) at reading levels III, IV, V, and VI in the normal 15-day-old fetus (N15₄-6).

<u>Reading Level</u>	<u>Staining Technique</u>	<u>C</u>	<u>NA</u>	<u>M</u>
III	H	4	4	2
	AB	4	4	2
	CV	3	3	1
IV	H	4	4	2
	AB	4	4	2
	CV	3	3	2
V	H	4	4	2
	AB	4	4	2
	CV	3	3	2
VI	H	4	2	2
	AB	4	2	2
	CV	3	1	1

Table V

The Hale reaction (H), alcian blue (AB), and cresyl violet (CV) staining values in the centra (C), neural arches (NA), and subspinal cord mesenchyme (M) at reading levels II, III, IV, and V in the normal 16-day-old fetus (N16₁₋₂).

<u>Reading Level</u>	<u>Staining Technique</u>	<u>C</u>	<u>NA</u>	<u>M</u>
II	H	4	4	3
	AB	4	4	3
	CV	4	4	2
III	H	4	4	3
	AB	4	4	3
	CV	4	4	2
IV	H	4	4	3
	AB	4	4	3
	CV	4	4	2
V	H	4	4	3
	AB	4	4	3
	CV	4	4	2

Table VI

The Hale reaction (H), alcian blue (AB), and cresyl violet (CV) staining values in the centra (C), neural arches (NA), and subspinal cord mesenchyme (M) at reading levels II, III, and IV in the 14-day-old fetus (E14₂-7) with a myeloschisis deformity.

<u>Lesion Level</u>	<u>Normal Reading Level</u>	<u>Staining Technique</u>	<u>C</u>	<u>NA</u>	<u>M</u>
1	I	H	3	2	1
		AB	3	1	2
		CV	2	1	1
2	II	H	3	1	0
		AB	3	0	1
		CV	2	0	0
3	II	H	3	0	0
		AB	1	2	1
		CV	0	2	0
4	II	H	3	0	0
		AB	2	0	1
		CV	1	0	0
5	III	H	2	1	1
		AB	1	0	1
		CV	1	0	0
6	III	H	2	1	2
		AB	2	1	2
		CV	1	0	0
7	IV	H	2	1	2
		AB	2	1	1
		CV	2	1	0

Table VII

The Hale reaction (H), alcian blue (AB), and cresyl violet (CV) staining values in the centra (C), neural arches (NA), and subspinal cord mesenchyme (M) at reading levels II, III, IV, and V in the 14-day-old fetus (E14₁₋₃) with a myeloschisis deformity.

<u>Lesion Level</u>	<u>Normal Reading Level</u>	<u>Staining Technique</u>	<u>C</u>	<u>NA</u>	<u>M</u>
1	II	H	3	2	2
		AB	3	3	2
		CV	2	2	1
2	III	H	2	2	1
		AB	2	1	1
		CV	1	1	0
3	III	H	2	0	0
		AB	2	1	1
		CV	1	0	0
4	IV	H	3	1	0
		AB	3	1	1
		CV	2	0	0
5	IV	H	3	1	1
		AB	3	2	2
		CV	2	0	1
6	V	H	3	2	2
		AB	3	2	2
		CV	3	1	1
7	V	H	3	2	2
		AB	3	2	2
		CV	2	1	1

Table VIII

The Hale reaction (H), alcian blue (AB), and cresyl violet (CV) staining values in the centra (C), neural arches (NA), and subspinal cord mesenchyme (M) at reading levels III, IV, V, and VI in the 14-day-old fetus (E14₃-5), sagittally-sectioned, with a myeloschisis deformity.

<u>Lesion Level</u>	<u>Normal Reading Level</u>	<u>Staining Technique</u>	<u>C</u>	<u>NA</u>	<u>M</u>
1	III	H	3	2	2
		AB	3	1	2
		CV	2	0	1
2	IV	H	2	0	0
		AB	2	0	1
		CV	0	0	0
3	IV	H	2	0	0
		AB	2	0	1
		CV	0	0	0
4	V	H	3	1	0
		AB	3	0	1
		CV	1	0	0
5	VI	H	3	1	2
		AB	3	1	2
		CV	2	0	1

Table IX

Hale reaction (H), alcian blue (AB), and cresyl violet (CV) staining values in the centra (C), neural arches (NA), and subspinal cord mesenchyme (M) at reading levels III, IV, V, and VI in the 15-day-old fetus (E15₆-11) with a myeloschisis deformity.

<u>Lesion Level</u>	<u>Normal Reading Level</u>	<u>Staining Technique</u>	<u>C</u>	<u>NA</u>	<u>M</u>
1	III	H	4	3	3
		AB	4	3	3
		CV	3	3	2
2	III	H	2	1	1
		AB	2	1	1
		CV	2	0	0
3	IV	H	3	0	0
		AB	3	1	0
		CV	2	0	0
4	V	H	4	2	0
		AB	3	2	2
		CV	3	1	0
5	VI	H	3	2	1
		AB	3	2	3
		CV	2	1	1

Table X

The Hale reaction (H), alcian blue (AB), and cresyl violet (CV) staining values in the centra (C), neural arches (NA), and subspinal cord mesenchyme (M) at reading levels III, IV, and V in the 15-day-old fetus (E15₇₋₁₁) with a myeloschisis deformity.

<u>Lesion Level</u>	<u>Normal Reading Level</u>	<u>Staining Technique</u>	<u>C</u>	<u>NA</u>	<u>M</u>
1	III	H	3	3	2
		AB	4	3	2
		CV	3	2	1
2	III	H	3	1	1
		AB	3	0	1
		CV	2	0	0
3	IV	H	3	0	0
		AB	3	1	1
		CV	2	0	0
4	IV	H	3	2	1
		AB	3	2	2
		CV	2	1	1
5	IV	H	3	2	2
		AB	3	2	2
		CV	2	1	1
6	V	H	3	2	2
		AB	3	2	2
		CV	2	1	1

Table XI

The Hale reaction (H), alcian blue (AB), and cresyl violet (CV) staining values in the centra (C), neural arches (NA), and subspinal cord mesenchyme (M) at reading levels III, IV, and V in the 15-day-old fetus (E15₆-5), sagittally-sectioned, with a myeloschisis deformity.

<u>Lesion Level</u>	<u>Normal Reading Level</u>	<u>Staining Technique</u>	<u>C</u>	<u>NA</u>	<u>M</u>
1	II	H	4	4	2
		AB	3	3	2
		CV	3	2	1
2	III	H	3	0	0
		AB	2	0	0
		CV	1	0	0
3	III	H	3	1	0
		AB	2	1	0
		CV	1	0	0
4	IV	H	3	2	0
		AB	2	2	1
		CV	2	1	0
5	V	H	4	2	2
		AB	2	2	2
		CV	2	1	1

Table XII

The Hale reaction (H), alcian blue (AB), and cresyl violet (CV) staining values in the centra (C), neural arches (NA), and subspinal cord mesenchyme (M) at reading levels II, III, IV, and V in the 16-day-old fetus (E16₄₋₅) with a myeloschisis deformity.

<u>Lesion Level</u>	<u>Normal Reading Level</u>	<u>Staining Technique</u>	<u>C</u>	<u>NA</u>	<u>M</u>
1	II	H	4	4	2
		AB	4	4	2
		CV	4	4	1
2	III	H	4	0	2
		AB	4	1	1
		CV	4	0	0
3	III	H	4	0	1
		AB	4	1	1
		CV	4	0	0
4	IV	H	4	1	1
		AB	4	1	0
		CV	4	0	0
5	IV	H	4	4	0
		AB	4	4	1
		CV	4	4	0
6	V	H	4	4	2
		AB	4	4	2
		CV	4	4	1
7	V	H	4	4	1
		AB	4	4	2
		CV	3	2	1

Table XIII

The Hale reaction (H), alcian blue (AB), and cresyl violet (CV) staining values in the centra (C), neural arches (NA), and subspinal cord mesenchyme (M) at reading levels II, III, and IV in the 16-day-old fetus (El6₄-2) with a myeloschisis deformity.

Lesion Level	Normal Reading Level	Staining Technique	C	NA	M
1	II	H	4	4	2
		AB	4	4	2
		CV	4	4	1
2	II	H	4	4	2
		AB	4	4	2
		CV	4	4	1
3	II	H	3	0	0
		AB	4	1	1
		CV	4	0	0
4	II	H	3	0	0
		AB	4	1	0
		CV	4	0	0
5	III	H	4	4	2
		AB	4	4	1
		CV	3	2	1
6	IV	H	4	3	2
		AB	4	4	2
		CV	4	2	1

Table XIV

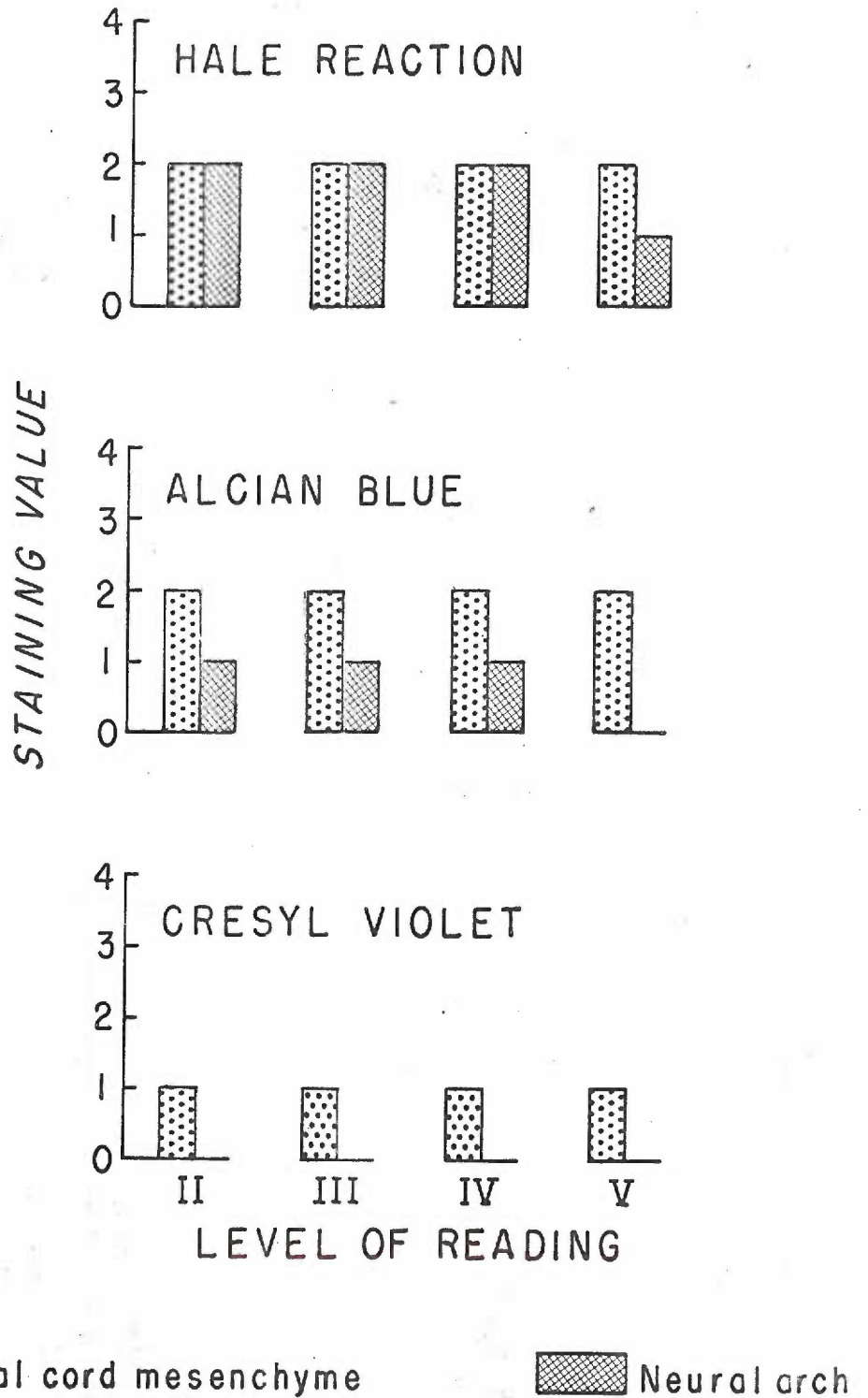
Tally by age of fetuses from noninjected mothers reviewed for normal study.

<u>Age</u>	<u>Section</u>	<u>Total Number Studied</u>
13	Cross	3
	Sagittal	3
14	Cross	2
	Sagittal	3
15	Cross	3
	Sagittal	3
16	Cross	2
	Sagittal	2
17	Cross	2
	Sagittal	2
18	Cross	1
	Sagittal	1

Graph 1

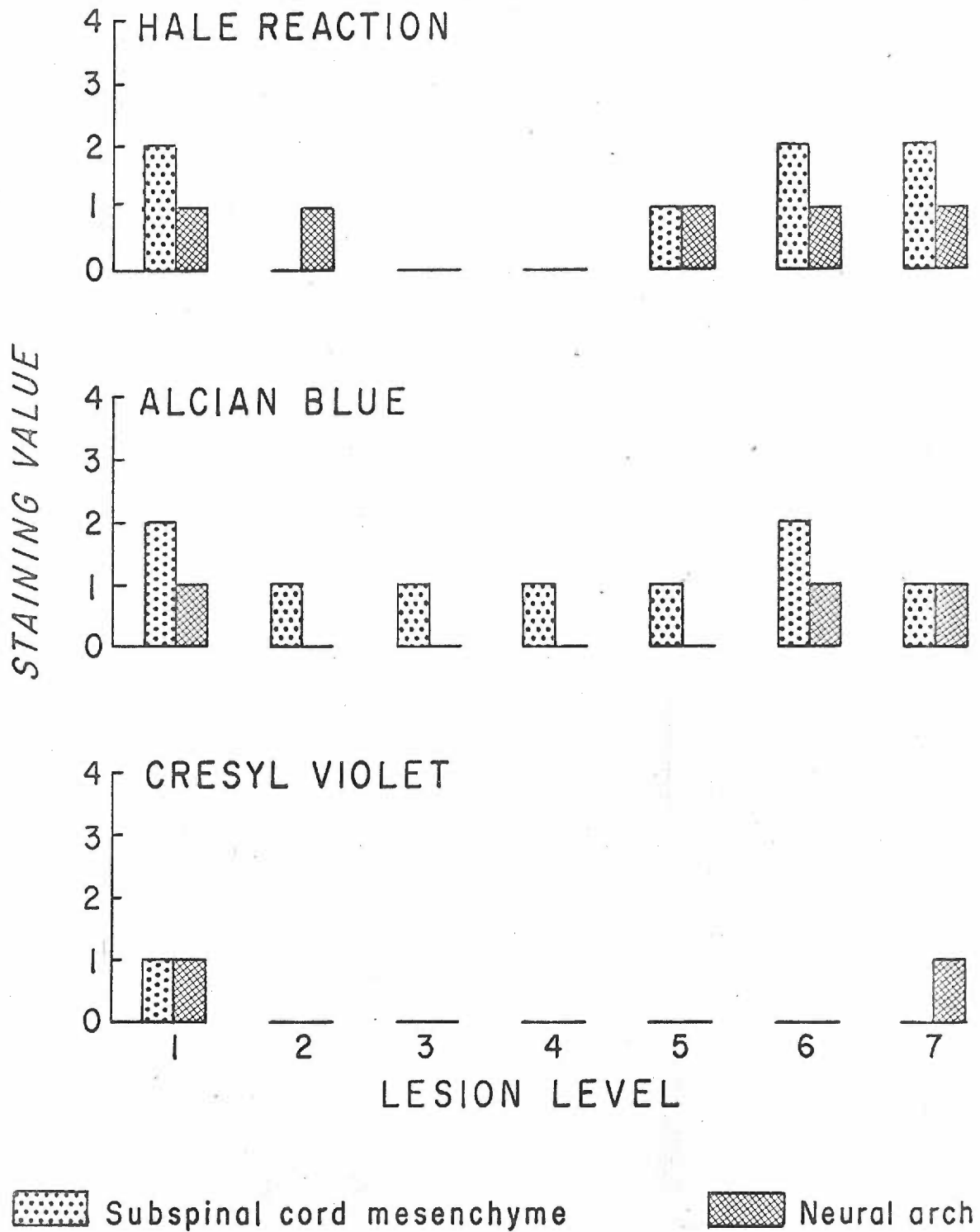
Normal fetus N14₁-6, described on pages 27-28 and tabulated in Table III. To compare with E14₂-7 and E14₃-5, consult text and Table II on page 77. Note that no changes in staining values occur until reading level 5 is reached.

N14,- 6



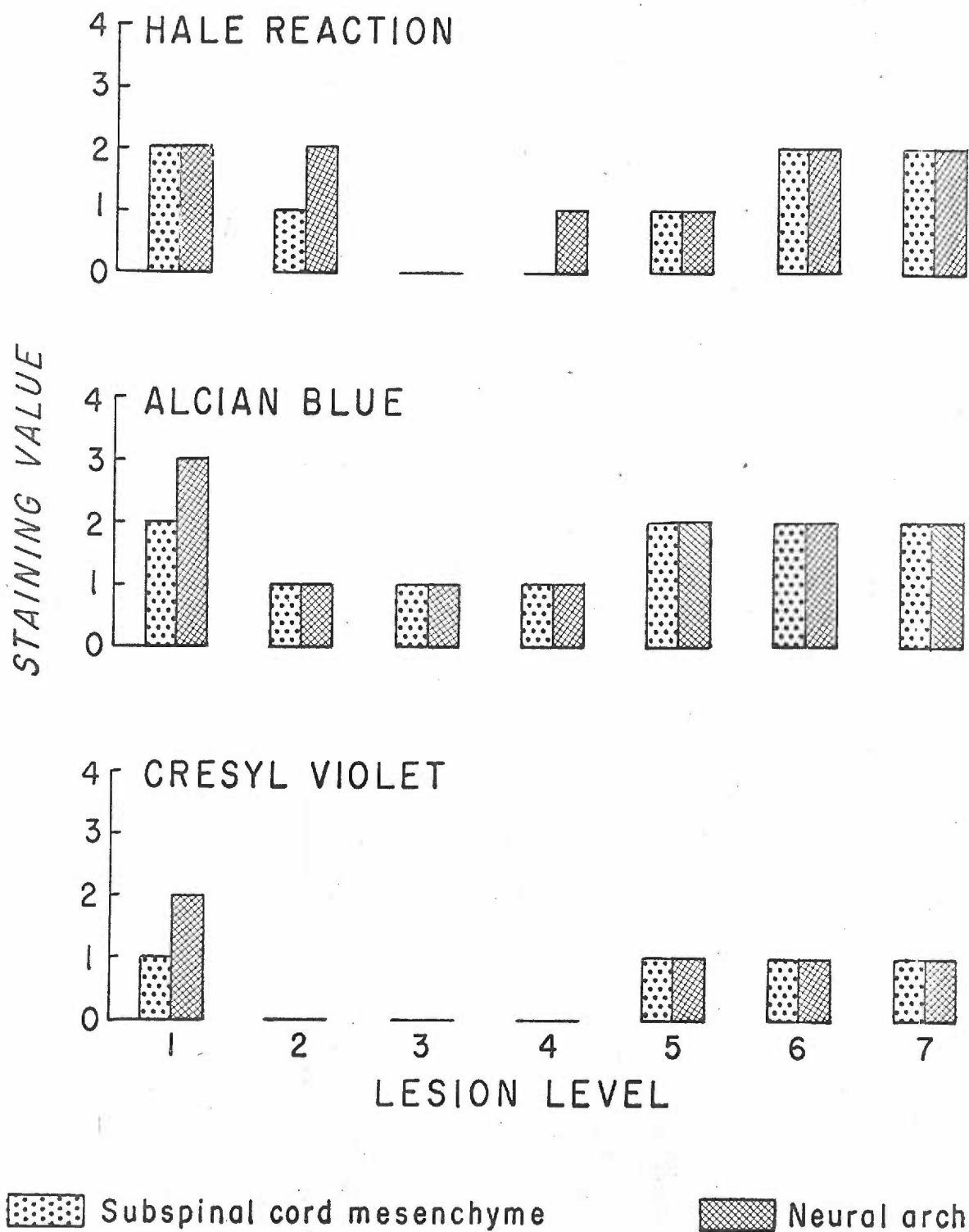
Graph 2

Fetus E14₂-7 with myeloschisis deformity. Note the decreased staining values for the subspinal cord mesenchyme and neural arches, especially at lesion levels 3 and 4. Refer to pages 38 through 41 for description and correlation with the proper graphs and tables.

E14₂-7

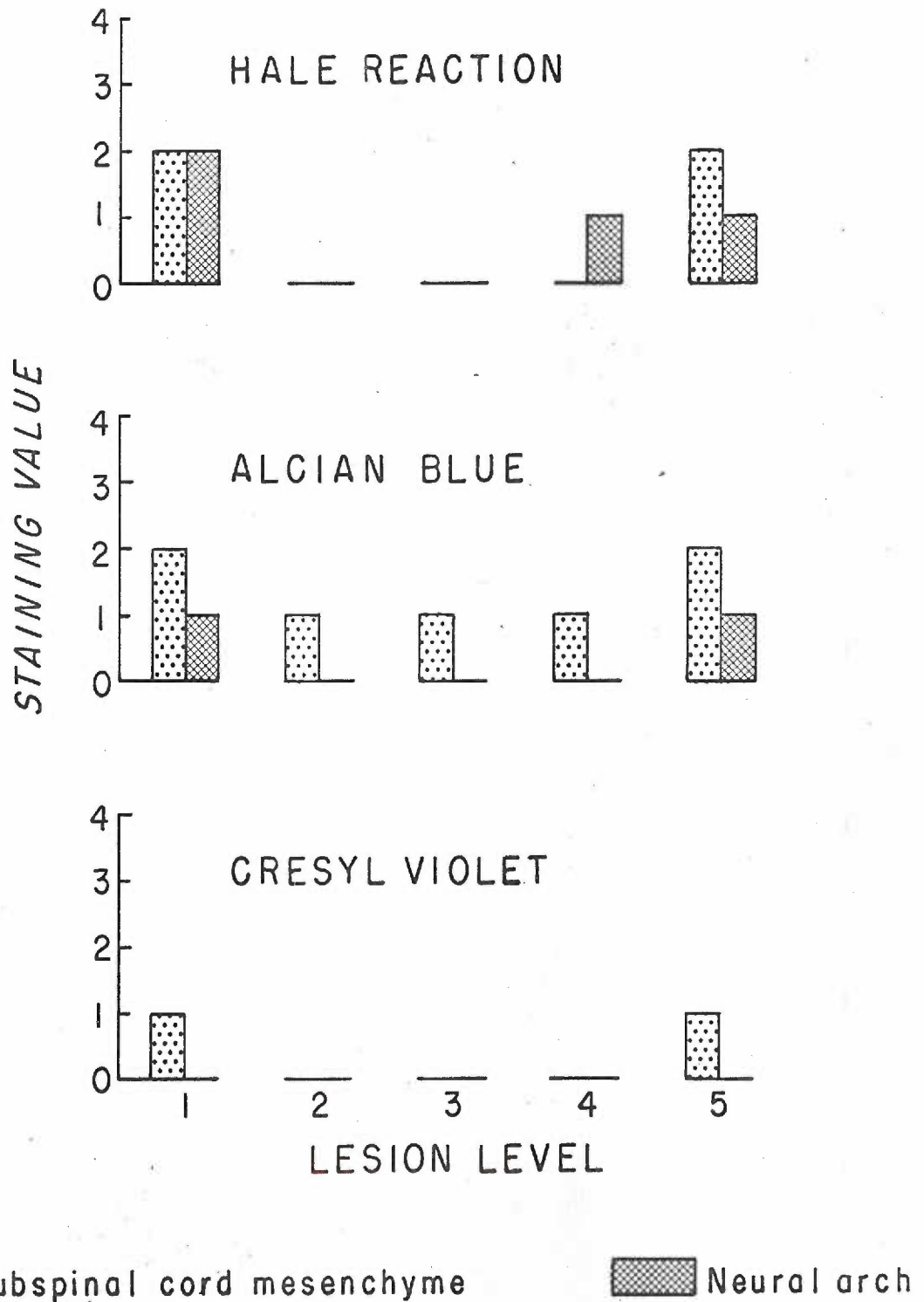
Graph 3

Fetus E14₁-3 with myeloschisis deformity. Note the decreased staining values for the subspinal cord mesenchyme and neural arches, especially at lesion levels 3 and 4. Refer to pages 41-42 for description and correlation with the proper normal graphs and tables.

E14_I-3

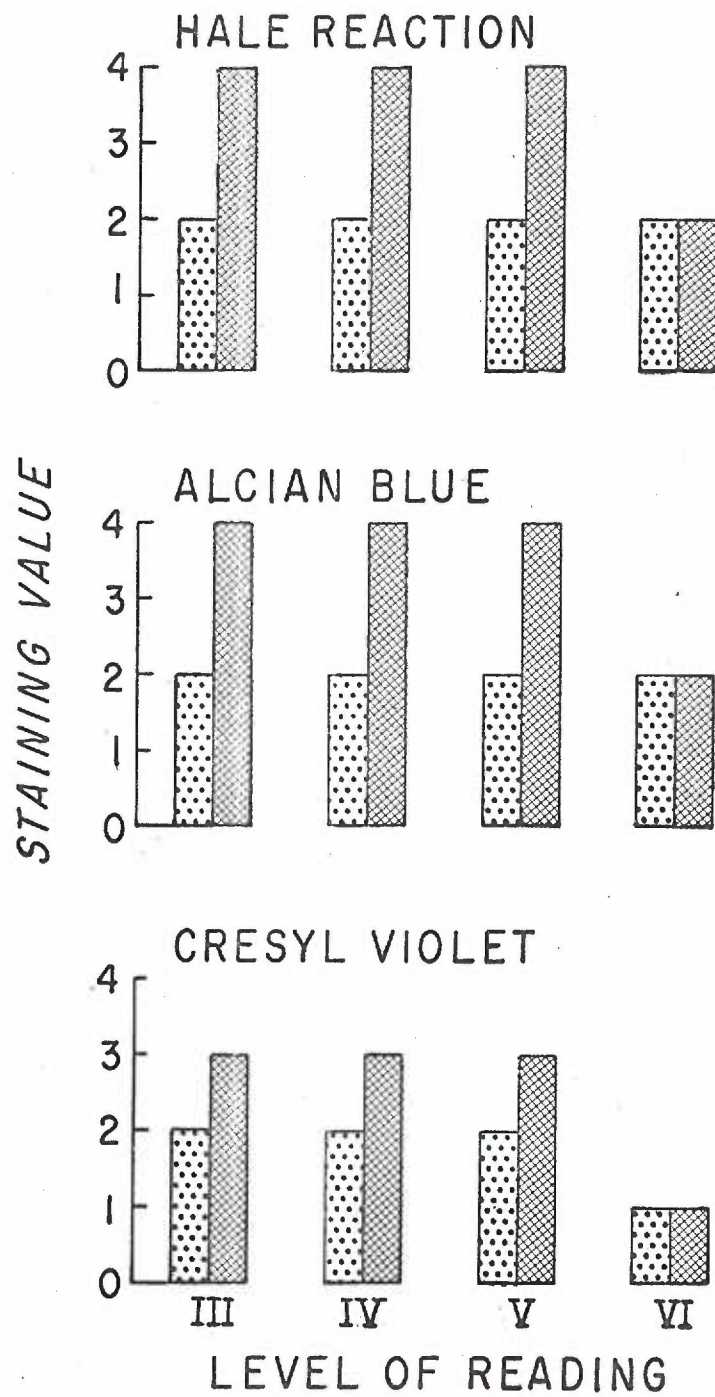
Graph 4


Fetus E14₃₋₅ (sagittal) with myeloschisis deformity. Note the decreased staining values for the subspinal cord mesenchyme and neural arches, especially at lesion levels 3, 4, and 5. Refer to pages 42-44 for description and correlation with the proper normal graphs and tables.

E14₃ - 5 SAGGITAL

Graph 5

Normal fetus N15₄-6, described on pages 28-30 and tabulated in Table IV. To compare with E15₆-11, E15₇-11, and E15₆-5, consult text and Table II on page 77. Note that no changes in staining values occur until reading level 6 is reached.

N15₄ -6

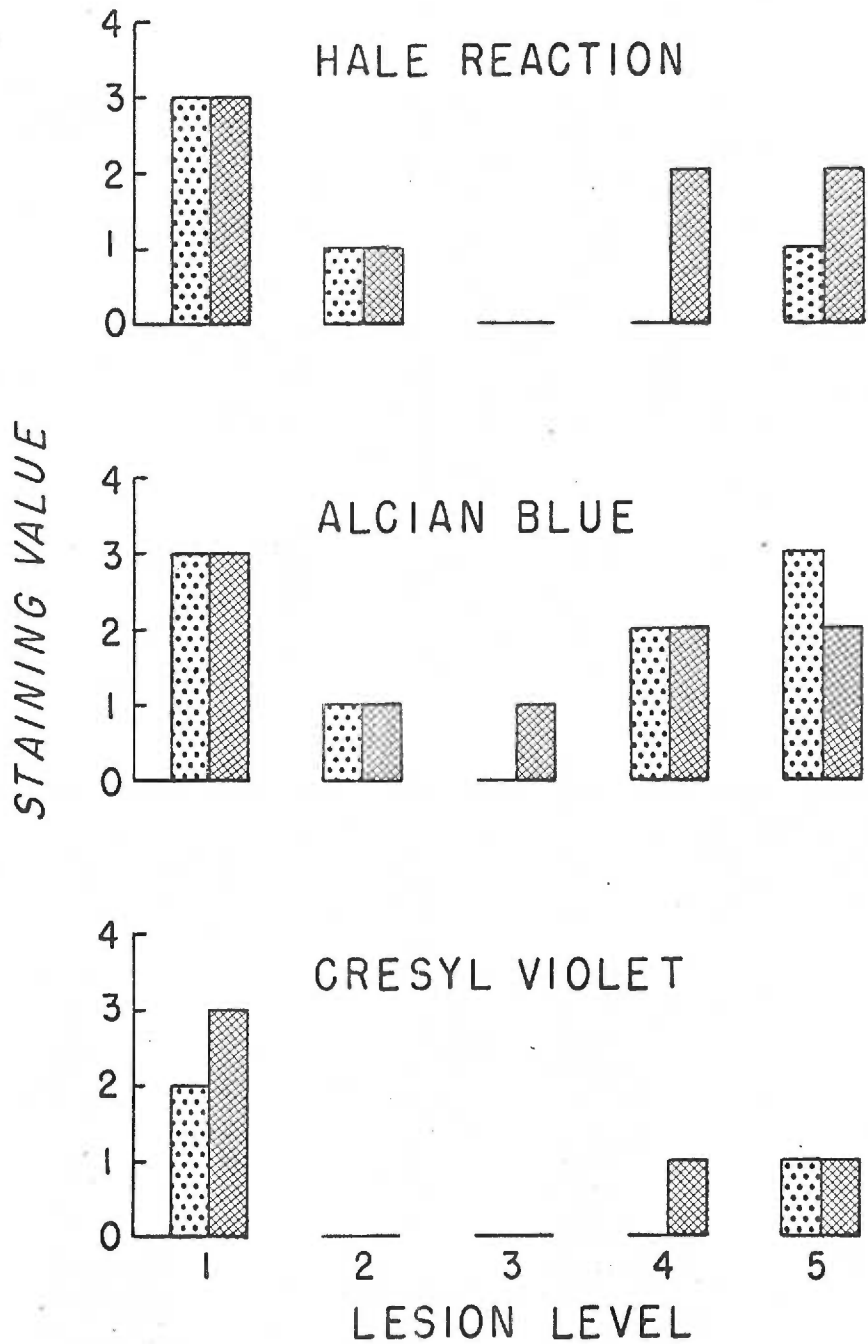
 Subspinal cord mesenchyme


 Neural arch

Graph 6

Fetus E15₆-11, with myeloschisis deformity. Note the decreased staining values for the subspinal cord mesenchyme and neural arches, especially at lesion levels 2 and 3. Refer to pages 44-46 for description and correlation with the proper graphs and tables.

E 15₆-11

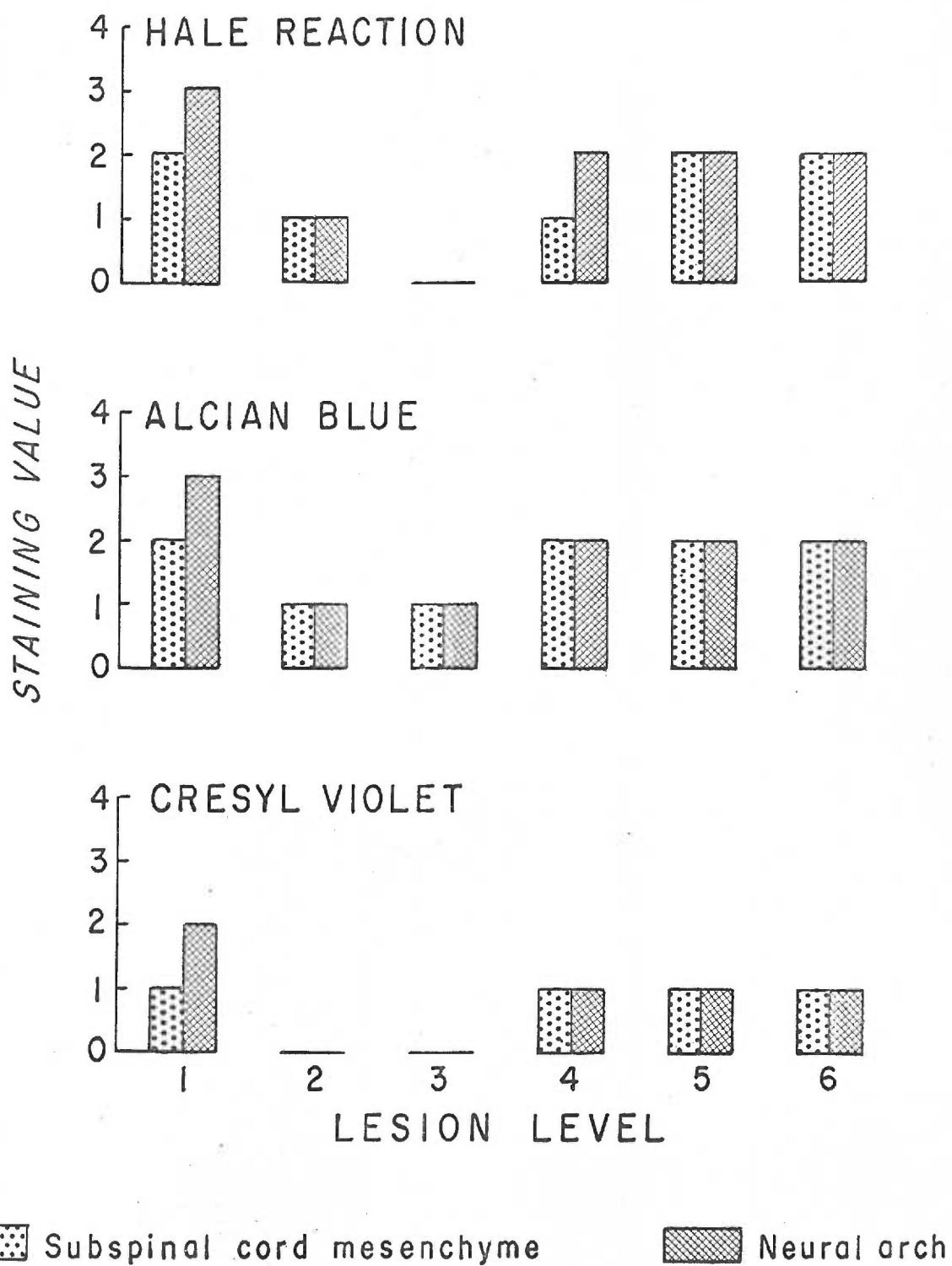


 Subspinal cord mesenchyme

 Neural arch

Graph 7

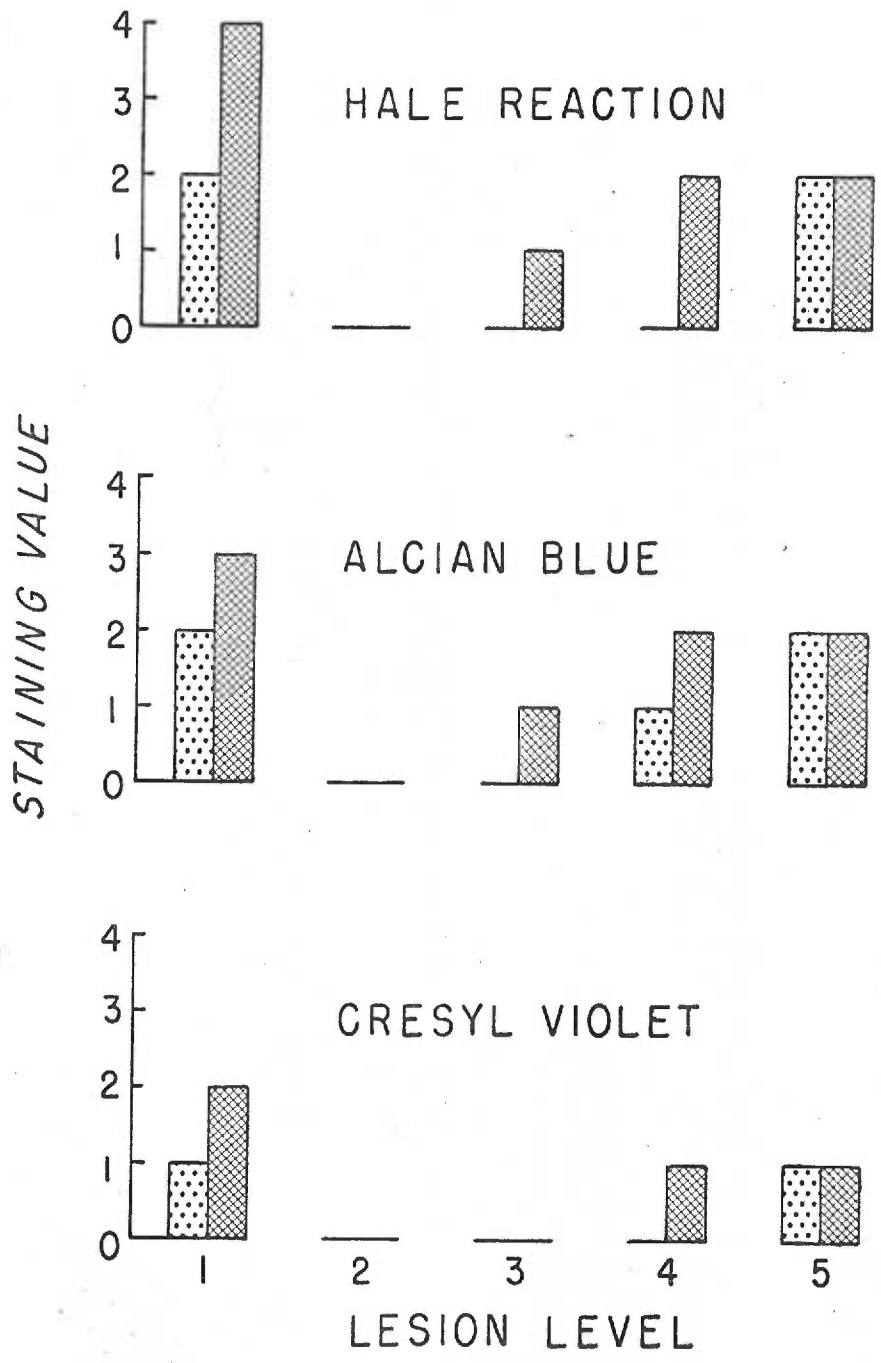
Fetus E15₇-11 with myeloschisis deformity. Note the decreased staining values from the subspinal cord mesenchyme and neural arches, especially at lesion levels 2 and 3. Refer to pages 46-48 for description and correlation with the proper graphs and tables.

E15₇-11

Graph 8

Fetus E156-⁵ with myeloschisis deformity. Note the decreased staining values for the subspinal cord mesenchyme and neural arches, especially at lesion levels 2 and 3. Refer to pages 48-50 for description and correlation with the proper graphs and tables.

E15₆-5 SAGGITAL

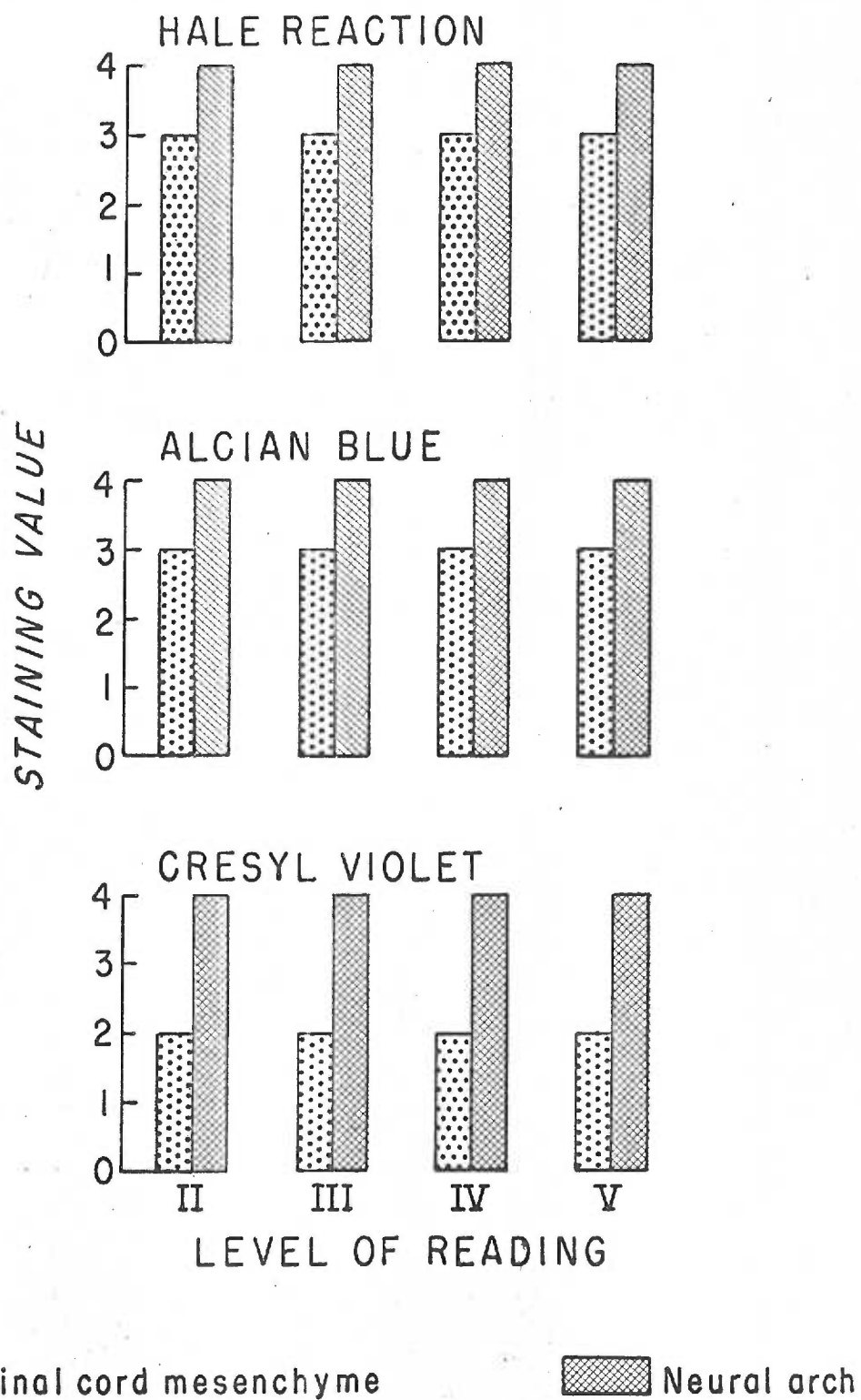


 Subspinal cord mesenchyme

 Neural arch

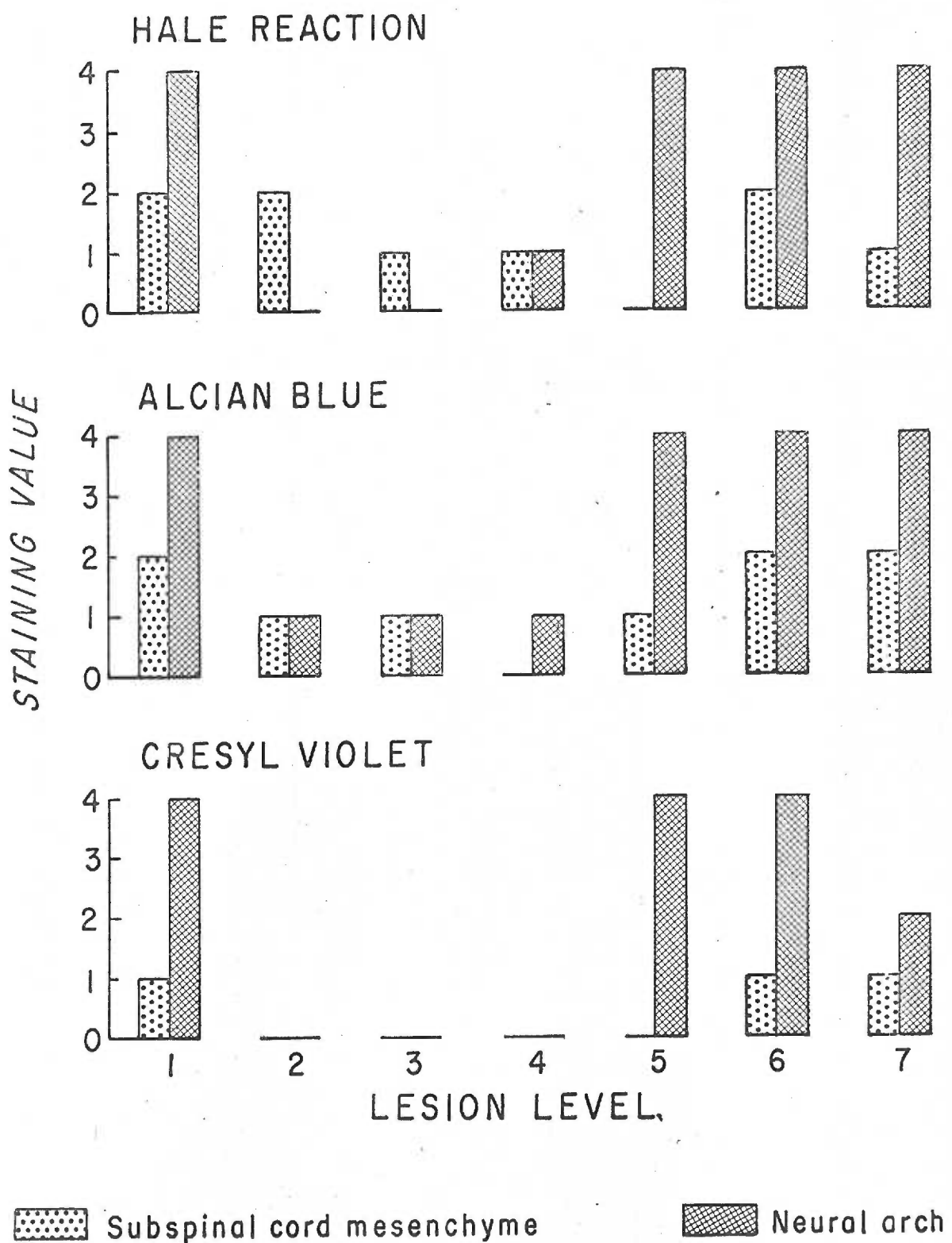
Graph 2

Normal fetus N16₁-2, described on pages 30-33 and tabulated on Table V. To compare with E16₄-5 and E16₄-2, consult text and Table II on page 77. Note that no changes in staining values occur through reading levels 2-5.

N16_I-2

Graph 10

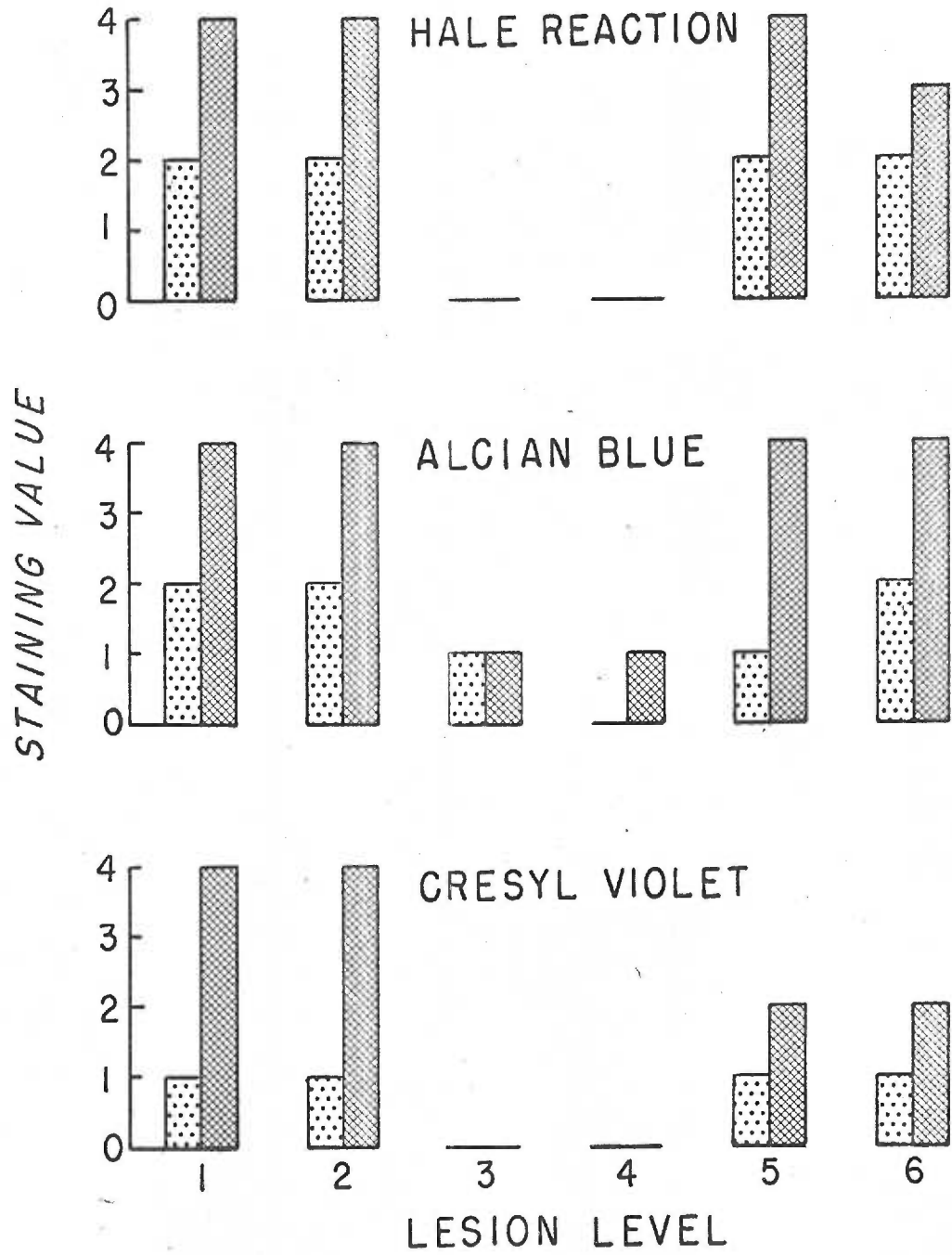
Fetus E16₄-5 with myeloschisis deformity. Note the decreased staining values for the subspinal cord mesenchyme and neural arches, especially at lesion levels 2, 3, and 4. Refer to pages 50-53 for description and correlation with the proper graphs and tables.


E16₄-5

Graph 11

Fetus E16₄-2 with myeloschisis deformity. Note the decreased staining values for the subspinal cord mesenchyme and neural arches, especially at lesion levels 3 and 4. Refer to pages 53-54 for description and correlation with the proper graphs and tables.

E 16₄ - 2



 Subspinal cord mesenchyme

 Neural arch

Plate I

Figures from normal fetus N15₄-2 at the levels of the anterior segments of the posterior limb buds. The lateral portion of the ventral spinal cord is seen in the upper part of the picture. Immediately below it is located the subspinal cord mesenchyme. A single portion of neural arch cartilage in the early cartilaginous phase can be seen in the lower portions of each picture. A portion of dorsal root ganglion can be seen at the mid-left margin.

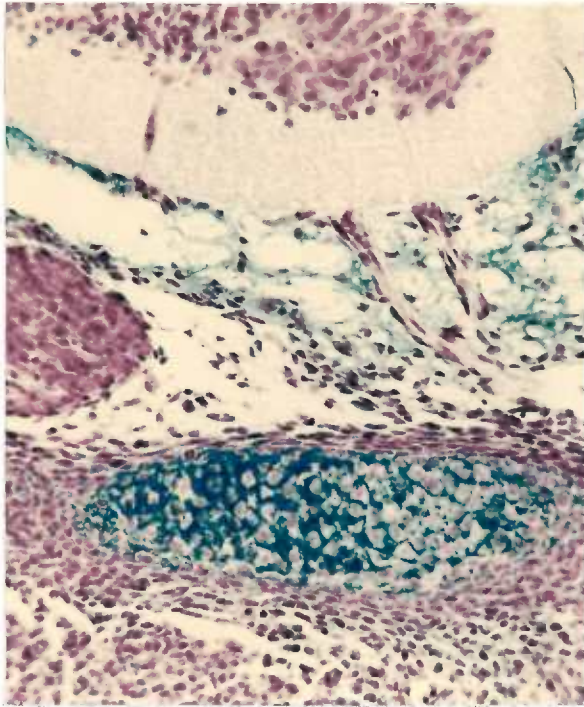
Figure A: Hale reaction. For description and discussion, refer to pages 29 and 55-56. (X170)

Figure B: Alcian blue stain. For description and discussion, refer to pages 29 and 56. (X170).

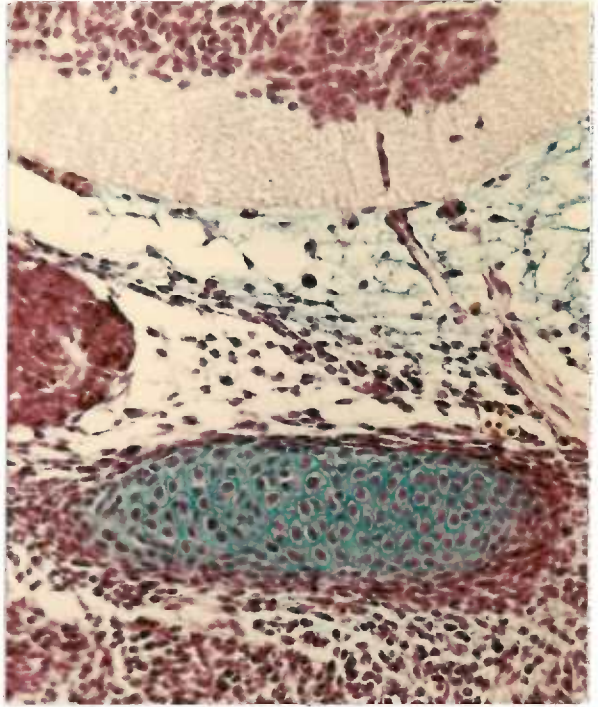
Figure C: Cresyl violet stain. For description and discussion, refer to pages 29 and 56. (X170)

Figure D: Periodic acid-Schiff stain. For description and discussion refer to pages 29 and 57-58. (X170)

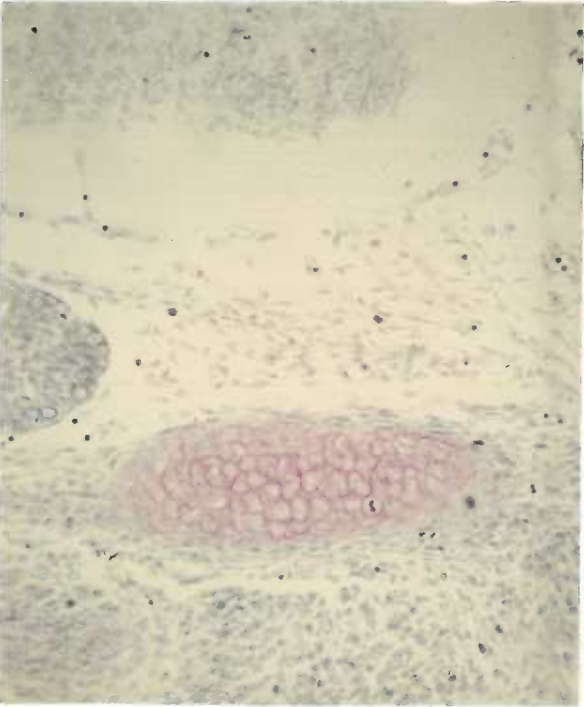
A



B



C



D

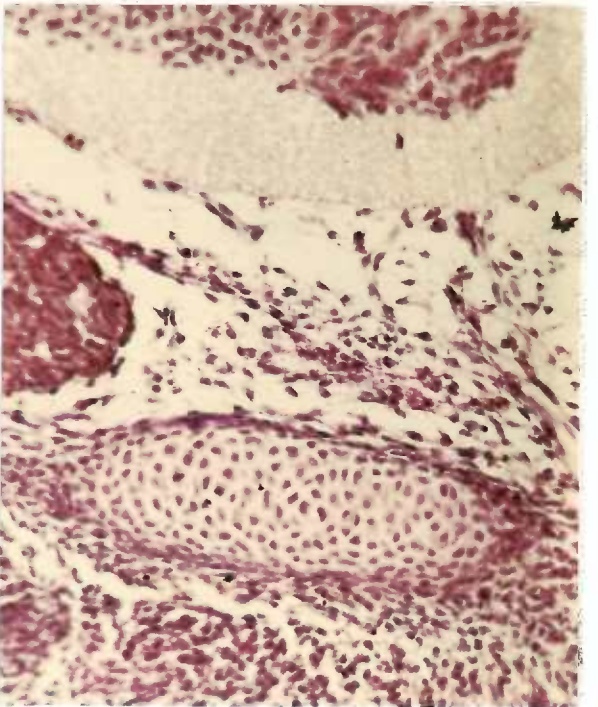


Plate II

Figures from normal fetus N18₁-7 at the levels of the anterior segments of the posterior limb buds. The lateral portion of the spinal cord lies outside the limits of the picture to the right. The large cartilage body, representing neural arch, is differentiated into two regions: the late cartilaginous phase above and the preosseous below. The neural arch arose from a centrum ventromedial to the picture. Staining in the myotomic tissue may be noted in the tissue at the left margin of the picture.

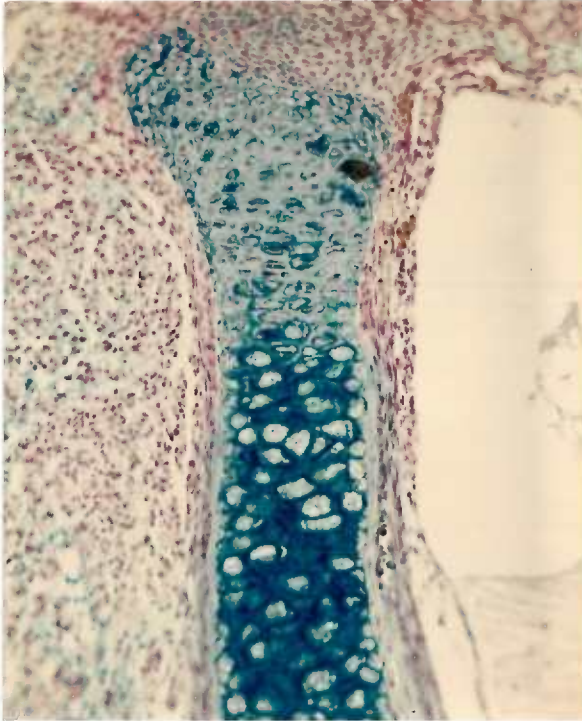
Figure A: Hale reaction. For description and discussion, refer to pages 35-36 and 55-56. (X130)

Figure B: Alcian blue stain. For description and discussion, refer to pages 36 and 56. (X130)

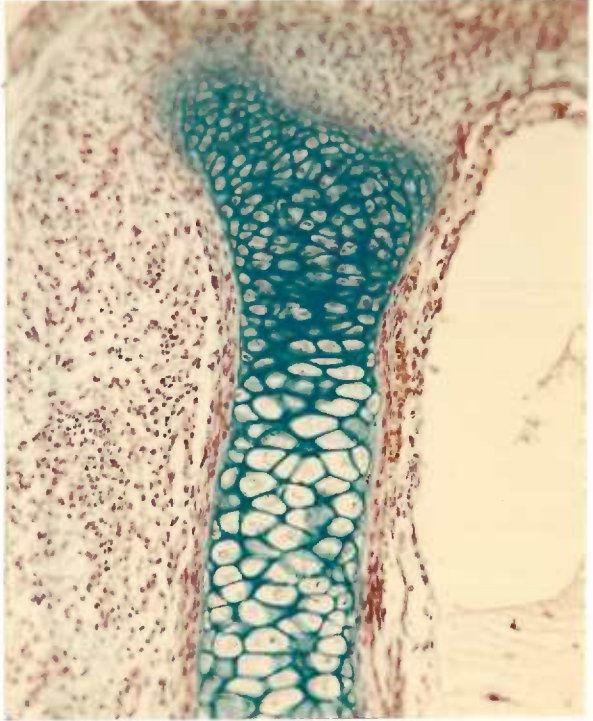
Figure C: Cresyl violet stain. For description and discussion, refer to pages 36-37 and 56. (X130)

Figure D: Periodic acid-Schiff stain. For description and discussion, refer to pages 37 and 57-58. (X130)

A



B



C



D

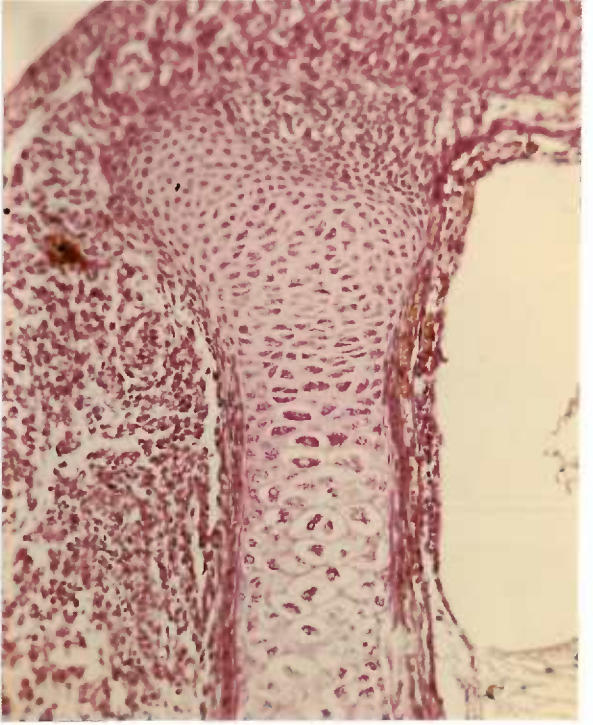
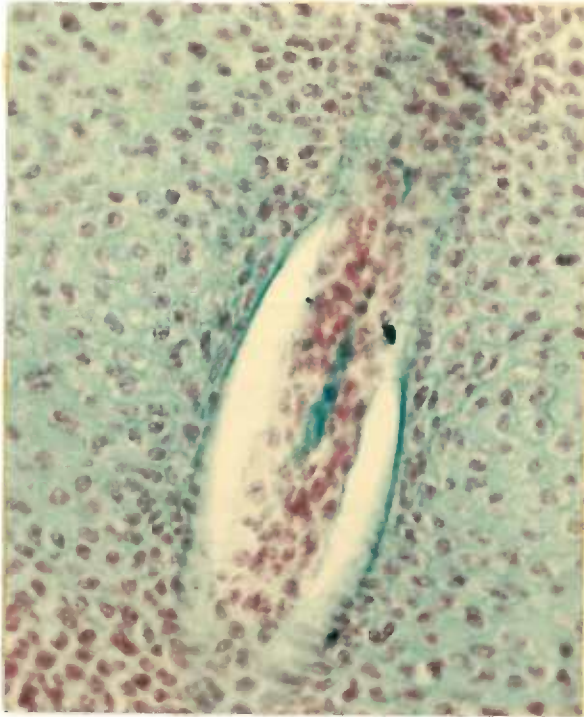


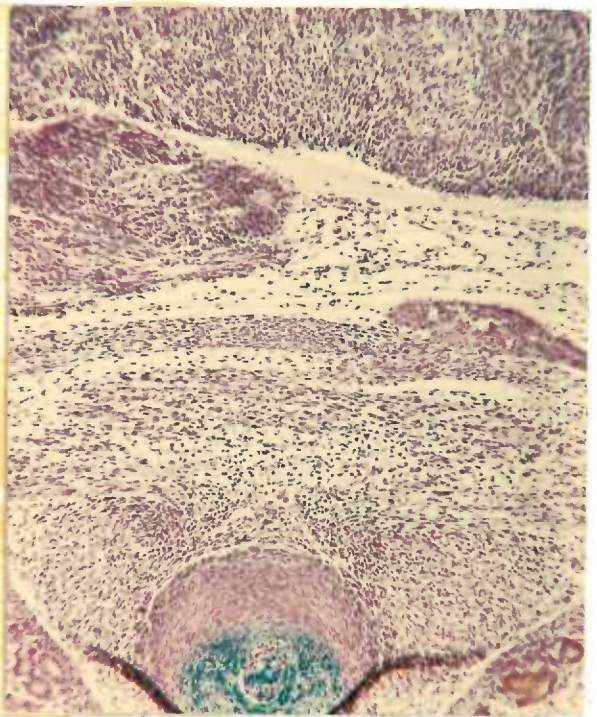
Plate III

- Figure A: Alcian blue stain. Rump of N15₄-2 cut in frontal section. A portion of notochord in surrounding precartilaginous phase centrum is depicted. Note the stained core of acellular material in the central notochord. The perinotochordal region is artifactually disrupted but increased staining may be observed at the margins. For description and discussion, refer to pages: notochord, 29 and 58-59; precartilaginous phase centrum, 30 and 55. (X370)
- Figure B: Hale reaction. Cross-section from midlesion of a myeloschisis deformity in E16₄-2 (page 54) is depicted. The deranged spinal cord tissue in the upper part of the picture overlies in order from dorsal to ventral, subspinal cord mesenchyme (unstained), sclerotomal cell layer (no neural arch - unstained), myotomic interlayers, and centrum around notochord. The centrum stained only in an oppositional nature around the notochord. Both the notochord and the centrum were displaced ventrally from their normal position. (X65)
- Figure C: Hale reaction. Midline sagittal section through a myeloschisis deformity in E14₃-5. The cranial part of the lesion is at the top of the picture, and the lesion is located at the mid-left margin. See page 42 of the text for description. (X34)
- Figure D: Hale reaction. Midline sagittal section through the anterior portion of a myeloschisis lesion in E15₆-5. Note the staining of the subspinal cord mesenchyme beneath the spinal cord on the left portion of the picture (cranial) and how it abruptly disappears at the margin of the lesion (right). (X65)

A



B



C



D

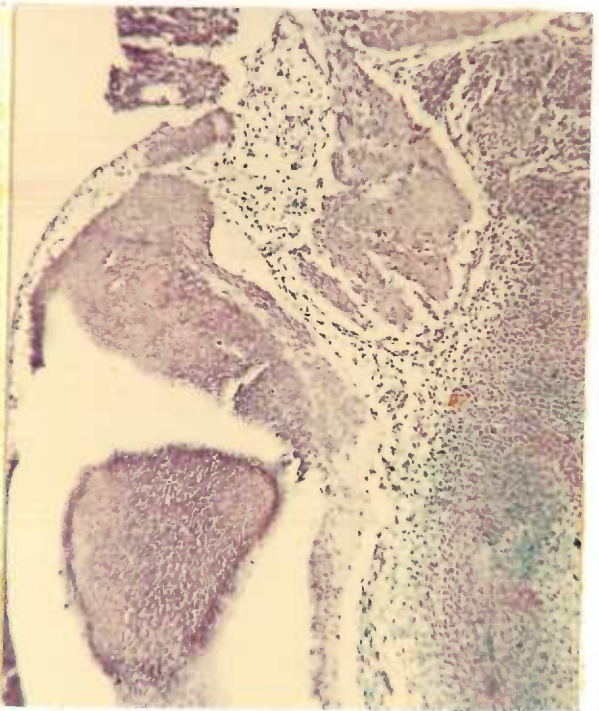


Plate IV

Fetus E14₂-7 with myeloschisis deformity is represented on the left in each photomicrograph. Description of each figure will be found in the text on pages 38 through 41. Data is represented in Table VIII and graph 4. Black and white photographs were made from slides stained by the Hale reaction. (X55)

Figure A: Lesion level 1.

Figure B: Lesion level 2.

Figure C: Lesion level 3.

Figure D: Lesion level 4. Compare with N14₁-2, Plate VII, Figure A.

Figure E: Lesion level 5.

Figure F: Lesion level 6. Compare with N14₁-2, Plate VII, Figure B.

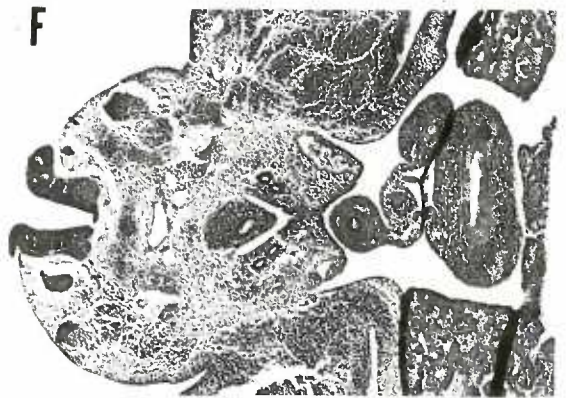
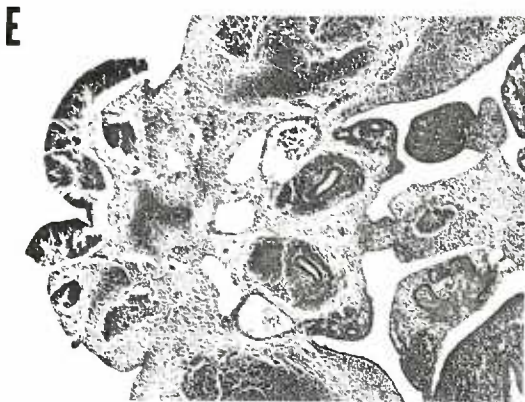
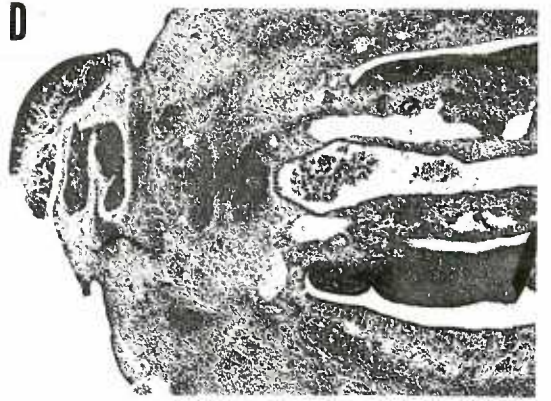
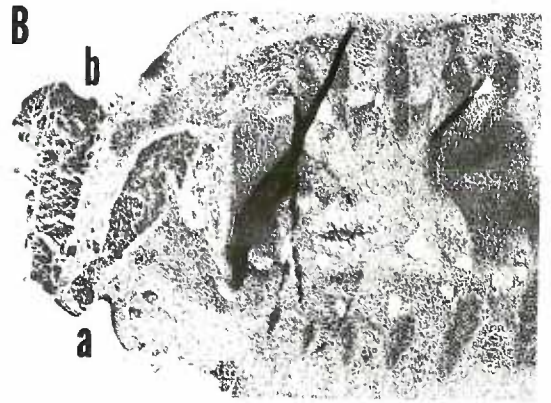
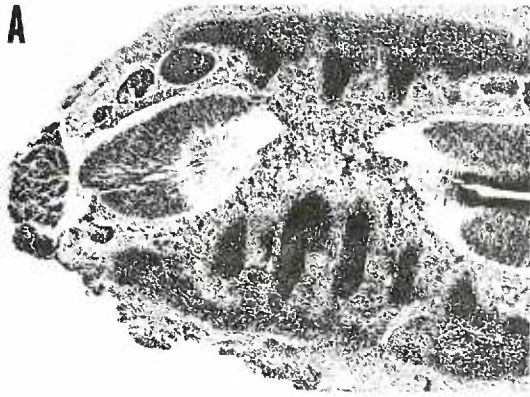


Plate V

Fetus E156-11 with myeloschisis deformity is represented by the following five photomicrographs. Description of each figure will be found in the text on pages 44 through 46. Data is represented in Table XI and graph 8. Black and white photographs were made from slides stained by the Hale reaction. (X35)

Figure A: Lesion level 1.

Figure B: Lesion level 2. Compare with N154-2, Plate VII, Figure C.

Figure C: Lesion level 3.

Figure D: Lesion level 4. Compare with N154-6, Plate VII, Figure D.

Figure E: Lesion level 5.

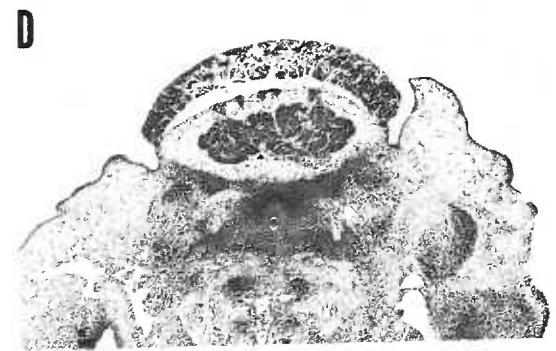
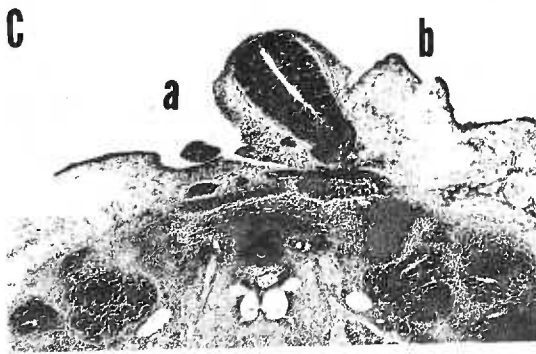
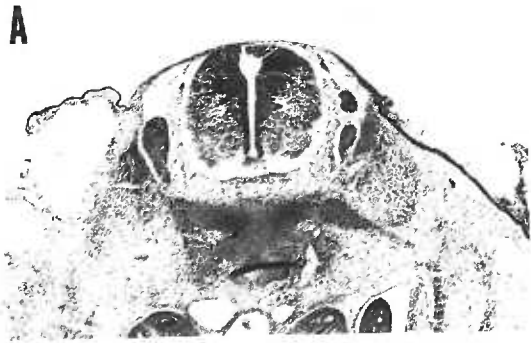


Plate VI

Fetus E16₁-5 with myeloschisis deformity is represented by the following six photomicrographs. Description of each figure will be found in the text on pages 50 through 53. Data is represented in Table XII and on graph 10. Black and white photographs were made from slides stained by the Hale reaction. (X45)

Figure A: Lesion level 1.

Figure B: Lesion level 2. Compare with N16₁-2, Plate VII, Figure E.

Figure C: Lesion level 3. Compare with N16₁-2, Plate VII, Figure E.

Figure D: Lesion level 4. Compare with N16₁-4, Plate VII, Figure F.

Figure E: Lesion level 5. Compare with N16₁-4, Plate VII, Figure F.

Figure F: Lesion level 6.

